Black hole perturbations in effective field theories of modified gravity

CANTATA
Cosmology and Astrophysics Network for Theoretical Advances and Training Actions

László Á. GERGELY
University of Szeged

based on:

C. Gergely, Z. Keresztes, L.Á. Gergely, PHYSICAL REVIEW D **99**, 104071 (2019)
R. Kase, L.Á. Gergely, S. Tsujikawa, PHYSICAL REVIEW D **90**, 124019 (2014)

4th Workgroup Meeting of COST Action CA-15117:
Cosmology and Astrophysics Network for Theoretical Advances and Training Actions (CANTATA)
7-10 October 2019, University of Tuzla, Bosnia and Herzegovina

Hungarian National Research Development and Innovation Office Grant NKFIH-123996
UNKP-19-3, UNKP-19-4 New National Excellence Programs of the Ministry of Human Capacities of Hungary

NATIONAL RESEARCH, DEVELOPMENT AND INNOVATION OFFICE

cost
EUROPEAN COOPERATION IN SCIENCE AND TECHNOLOGY

Nemzeti Kiválóság Program

Isaac Newton: the first successful gravity theory

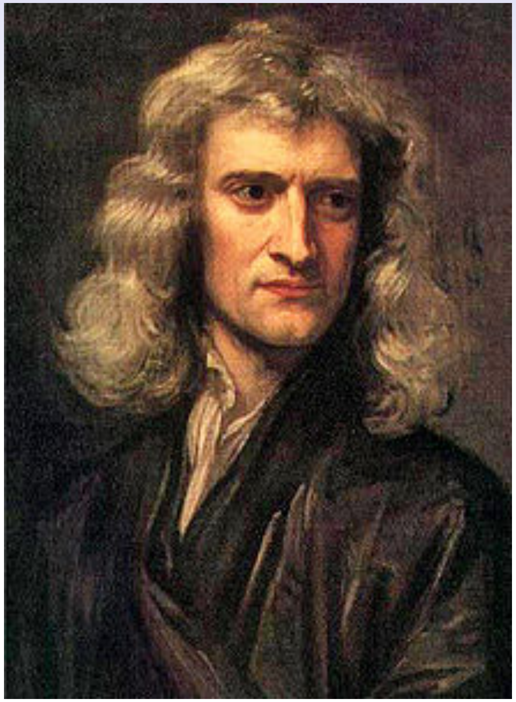

1642 – 1726/7

Philosophiae Naturalis Principia Mathematica (1687)

Establishes classical mechanics

Three laws of motion

Universal gravity theory

Derives Kepler's laws

Develops Calculus

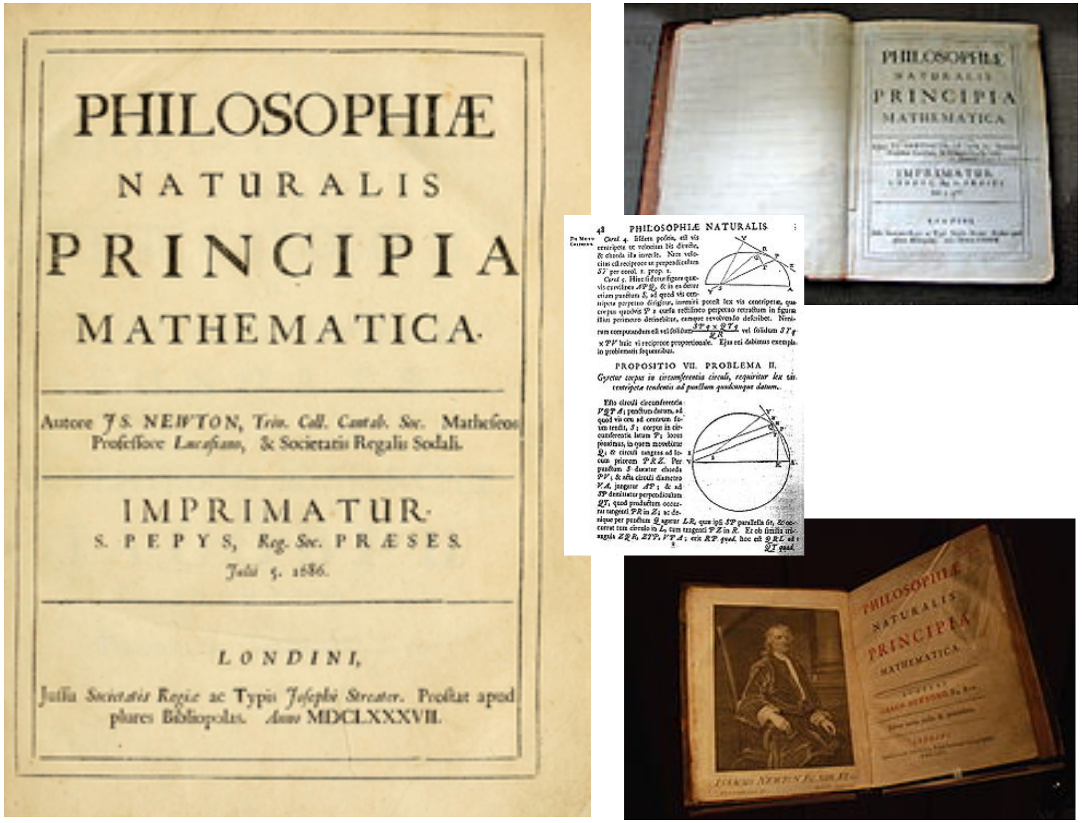

PHILOSOPHIÆ
NATURALIS
PRINCIPIA
MATHEMATICA.

Autore J S. NEWTON, *Trin. Coll. Cantab. Soc.* Matheſeos
Profeſſore *Lucaſiano*, & Societatis Regalis Sodali.

IMPRIMATUR.
S. PEPYS, *Reg. Soc.* PRÆSES.
Julii 5. 1686.

LONDINI,
Juſſu Societatis Regiæ ac Typis *Joſephi Streater*. Proſtat apud
plures Bibliopolas. *Anno* MDCLXXXVII.

Newton's gravity theory: strengths and limitations

Strengths:

Unique logical framework for both the celestial and everyday life motions

Poweful tool, allowing Le Verrier to predict the planet Neptune from the motion of the planet Uranus

Remarkably precise on the Earth (for weak gravity and slow motions)

$$\varepsilon = \frac{Gm}{c^2 r} \approx \frac{v^2}{c^2} \ll 1$$

Simple: one single scalar field

Limitations:

Assumes aether

The motion of the planets deviates from the Newtonian prediction (excess in the perihelion shift)

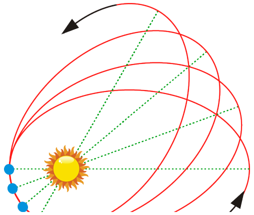

Not precise enough even on the Earth if one desires to use GPS

its accuracy of 15 m requires 50 ns temporal precision

SR: time dilation
-7 μs / day

GR: gravitational blueshift
45 μs / day

Combined Inaccuracy of
11.4 km / day

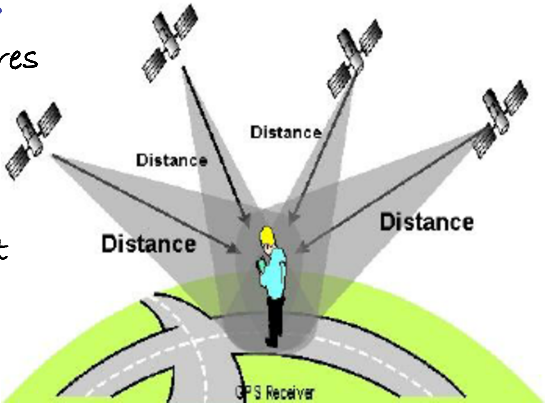

Infinite propagation speed

General relativity, Einstein's gravity theory

1. Matter tells space-time how to curve (Einstein equation)

$$R_{\mu\nu} - \frac{1}{2}R\, g_{\mu\nu} + \Lambda\, g_{\mu\nu} = \frac{8\pi G}{c^4} T_{\mu\nu}$$

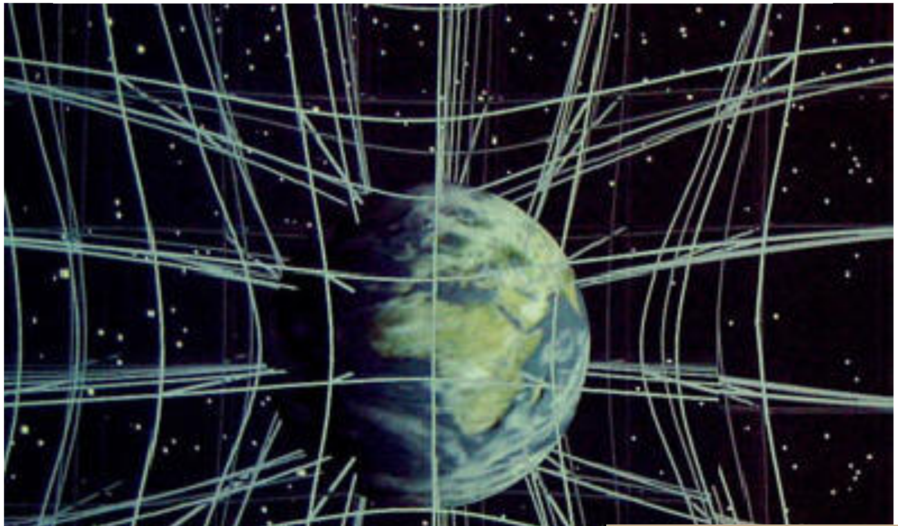

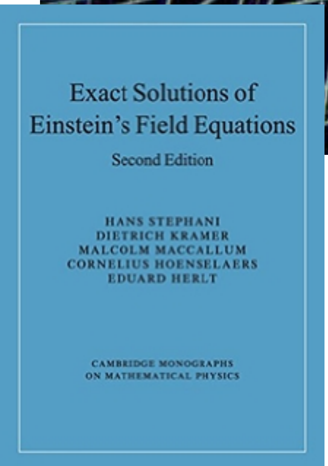

Exact Solutions of
Einstein's Field Equations
Second Edition

HANS STEPHANI
DIETRICH KRAMER
MALCOLM MACCALLUM
CORNELIUS HOENSELAERS
EDUARD HERLT

CAMBRIDGE MONOGRAPHS
ON MATHEMATICAL PHYSICS

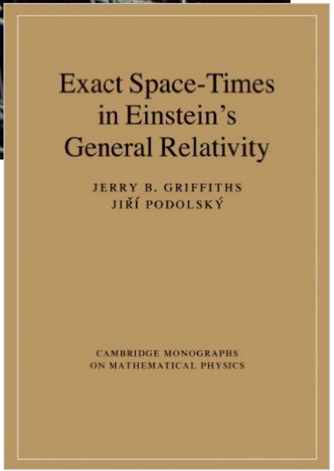

Exact Space-Times
in Einstein's
General Relativity

JERRY B. GRIFFITHS
JIŘÍ PODOLSKÝ

CAMBRIDGE MONOGRAPHS
ON MATHEMATICAL PHYSICS

2. Space-time tells matter, how to move (geodetic equation)

$$\frac{d^2x^\mu}{ds^2} = -\Gamma^\mu{}_{\alpha\beta}\frac{dx^\alpha}{ds}\frac{dx^\beta}{ds}$$

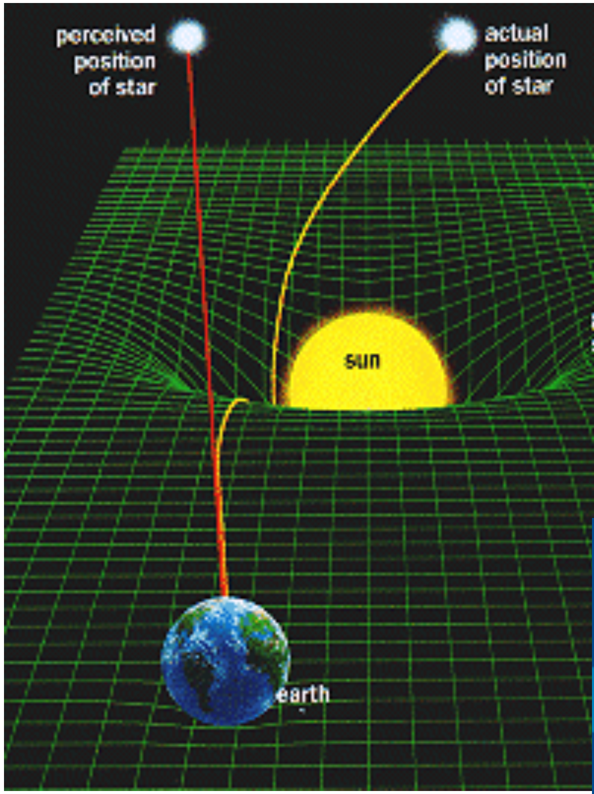

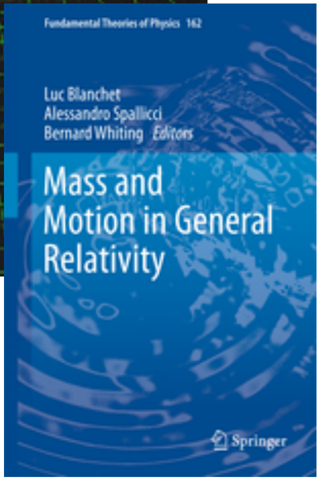

Fundamental Theories of Physics 162

Luc Blanchet
Alessandro Spallicci
Bernard Whiting *Editors*

Mass and
Motion in General
Relativity

Springer

The success of General Relativity

Solar System & other tests

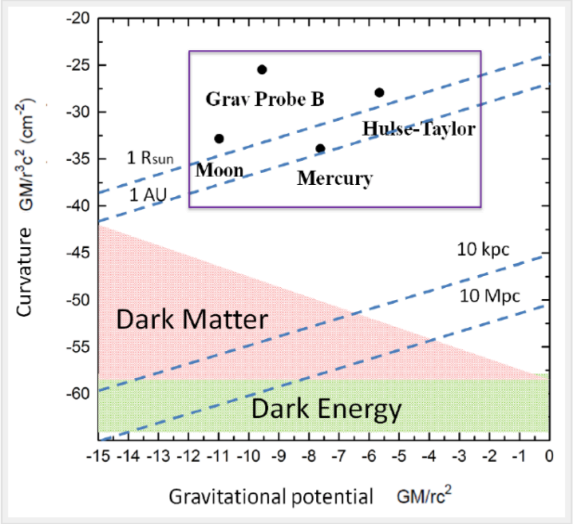

Fig 1: Tests of General Relativity on various scales. The vertical axis is the spacetime curvature and the horizontal axis is the gravitational potential. The blue dotted lines indicate typical length scales. Modified from Psaltis arXiv:0806.1531. GR is well tested at solar system scales and also by binary pulsars (within the purple box). However, outside this region, gravity is not tested by conventional methods.

www.icg.port.ac.uk/cosmological-tests-of-gravity/

Hulse-Taylor pulsar

Comparison between observations of the binary pulsar PSR1913+16, and the prediction of general relativity based on loss of orbital energy via gravitational waves

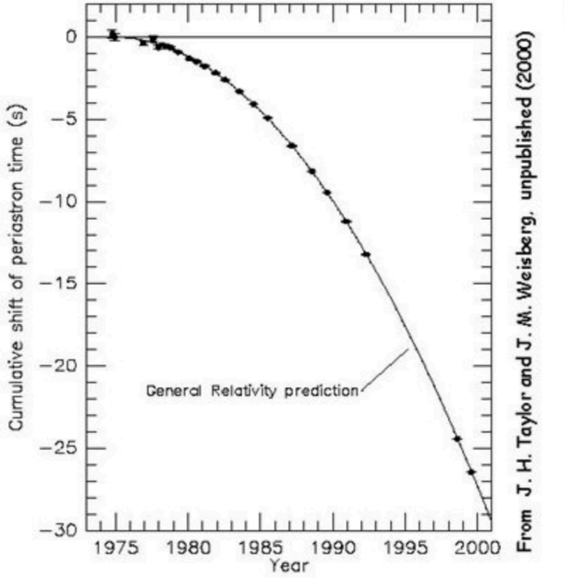

40s change in 30 years!! $(4x10^{-8})$

Gravity Probe B

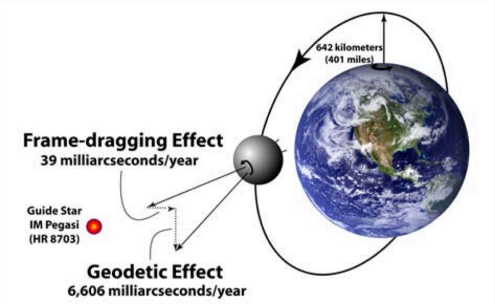

Everitt, C.W.F.; Parkinson, B.W. (2009). "Gravity Probe B Science Results—NASA Final Report"

Double pulsar

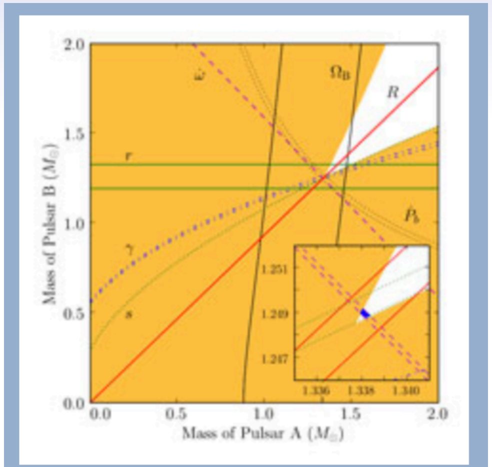

Mass-mass diagram illustrating the present tests constraining general relativity in the double pulsar PSR J0737-3039A/B. Because observations are consistent with general relativity, all lines intersect at common values of masses. Shaded orange regions are unphysical solutions because sin $i \leq 1$, where i is the orbital inclination. The mass ratio, R, and five post-Keplerian parameters (s and r, Shapiro delay shape and range; ω, periastron advance; $\dot{P}_b$, orbital period decay due to the emission of gravitational waves; and γ, gravitational redshift and time dilation) were reported by Kramer et al. (2006). The spin precession rate of pulsar B, Ω_B, yields a new constraint on the mass-mass diagram.

https://www.nrao.edu/news/newsletters/enews/enews_1_2/einstein.shtml

The success of General Relativity

Network of second generation gravitational wave observatories

Advanced LIGO, Hanford, USA, 4km

Advanced LIGO, Livingston, USA, 4km

Advanced Virgo, Cascina, Italy, 3km

KAGRA, Kamioke, Japan, 3km

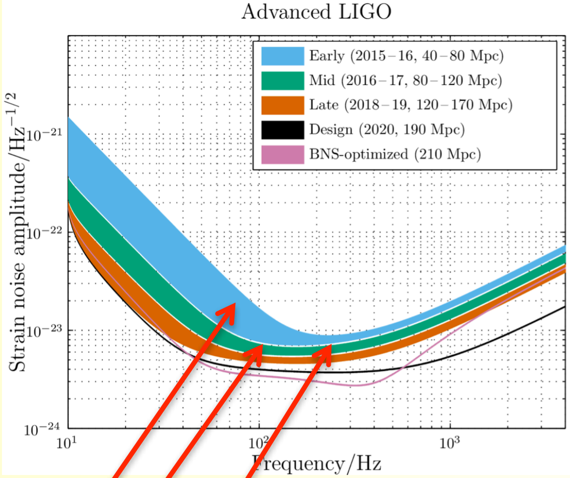

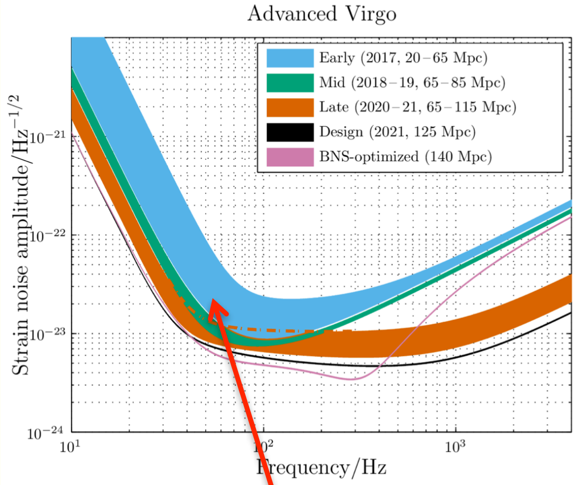

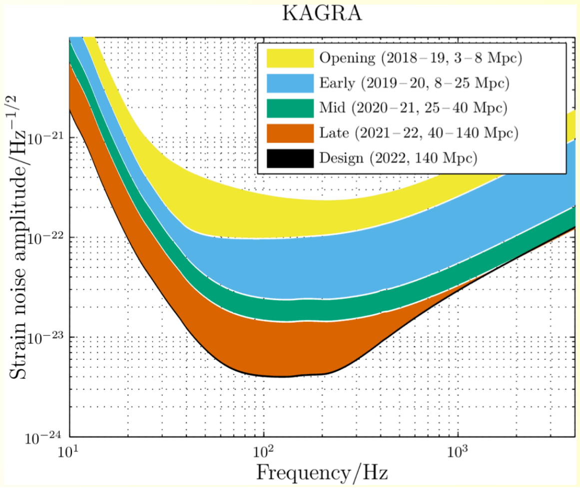

GW150915	GW151012	GW151226	O1
GW170104	GW170608	GW170729	O2
GW170809	GW170814	GW170817	O2
GW170818		GW170823	

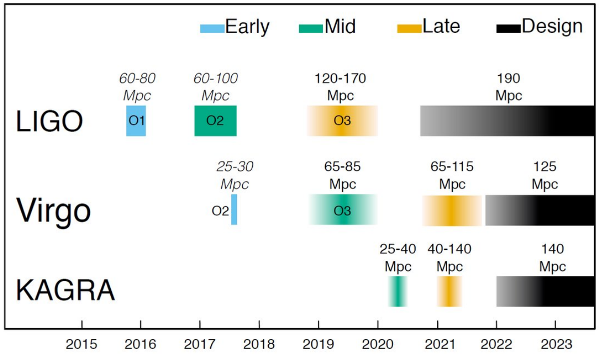

The success of General Relativity: Gravitational waves

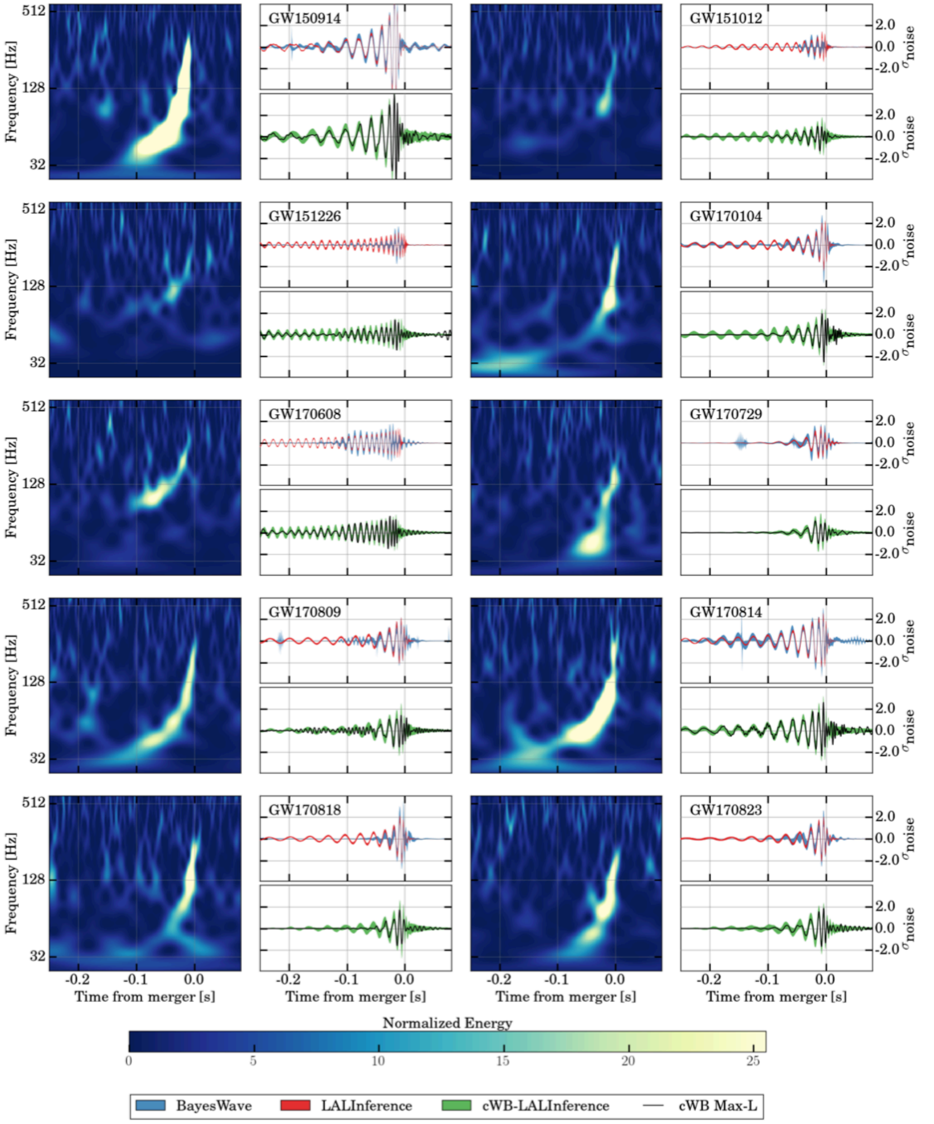

FIG. 10. Time-frequency maps and reconstructed signal waveforms for the ten BBH events. Each event is represented with three panels showing whitened data from the LIGO detector where the higher SNR was recorded. The first panel shows a normalized time-frequency power map of the GW strain. The remaining pair of panels shows time domain reconstructions of the whitened signal, in units of the standard

O1 and O2

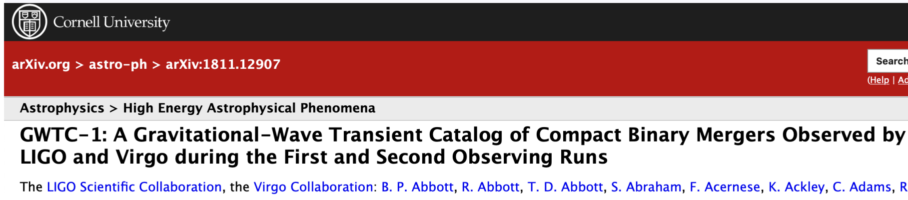
Cornell University

arXiv.org > astro-ph > arXiv:1811.12907

Astrophysics > High Energy Astrophysical Phenomena

GWTC-1: A Gravitational-Wave Transient Catalog of Compact Binary Mergers Observed by LIGO and Virgo during the First and Second Observing Runs

The LIGO Scientific Collaboration, the Virgo Collaboration: B. P. Abbott, R. Abbott, T. D. Abbott, S. Abraham, F. Acernese, K. Ackley, C. Adams, R

BNS: GW170817

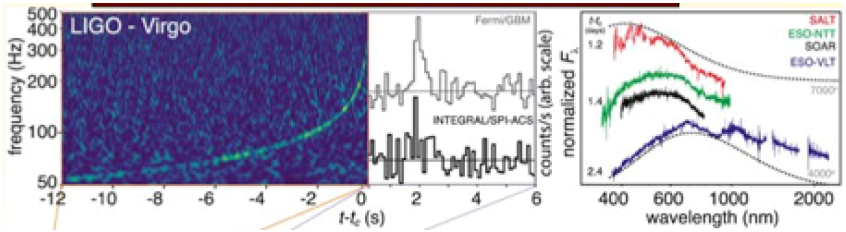

O3

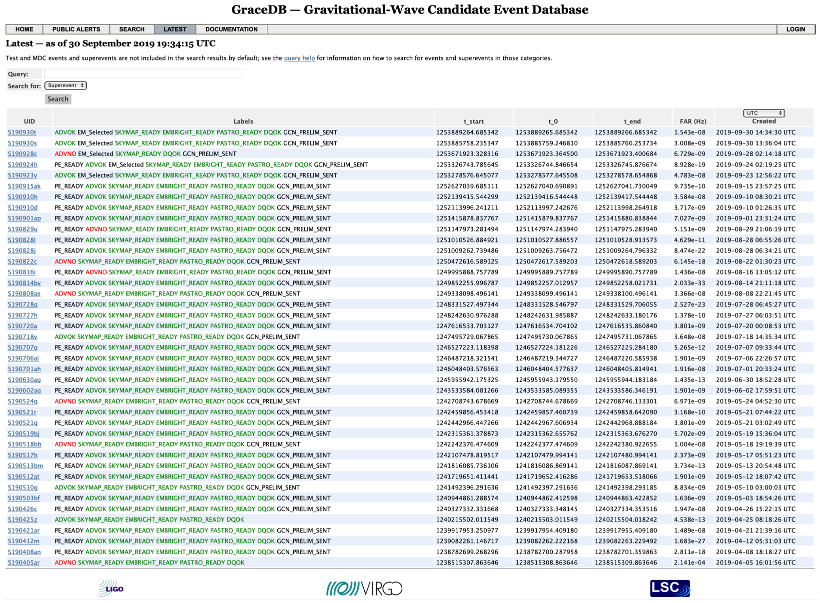
GraceDB — Gravitational-Wave Candidate Event Database

Latest — as of 30 September 2019 19:34:15 UTC

Test and MDC events and superevents are not included in the search results by default; see the query help for information on how to search for events and superevents in those categories.

Query:
Search for: Superevent

UID	Labels	t_start	t_0	t_end	FAR (Hz)	Created
S190930t	ADVOK EM_Selected SKYMAP_READY EMBRIGHT_READY PASTRO_READY DQOK GCN_PRELIM_SENT	1253889264.685342	1253889265.685342	1253889266.685342	1.543e-08	2019-09-30 14:34:30 UTC
S190930s	ADVOK EM_Selected SKYMAP_READY EMBRIGHT_READY PASTRO_READY DQOK GCN_PRELIM_SENT	1253885758.235347	1253885759.246810	1253885760.253734	3.008e-09	2019-09-30 13:36:04 UTC
S190928c	ADVNO EM_Selected SKYMAP_READY DQOK GCN_PRELIM_SENT	1253671923.328316	1253671923.364500	1253671923.400684	6.729e-09	2019-09-28 02:14:18 UTC
S190924h	PE_READY ADVOK EM_Selected SKYMAP_READY EMBRIGHT_READY PASTRO_READY DQOK GCN_PRELIM_SENT	1253326743.785645	1253326744.846654	1253326745.876674	8.928e-19	2019-09-24 02:19:25 UTC
S190923y	ADVOK EM_Selected SKYMAP_READY EMBRIGHT_READY PASTRO_READY DQOK GCN_PRELIM_SENT	1253278576.645077	1253278577.645508	1253278578.654868	4.783e-08	2019-09-23 12:56:22 UTC
S190915ak	PE_READY ADVOK SKYMAP_READY EMBRIGHT_READY PASTRO_READY DQOK GCN_PRELIM_SENT	1252627039.685111	1252627040.690891	1252627041.730049	9.735e-10	2019-09-15 23:57:25 UTC
S190910h	PE_READY ADVOK SKYMAP_READY EMBRIGHT_READY PASTRO_READY DQOK GCN_PRELIM_SENT	1252139415.544299	1252139416.544448	1252139417.544448	3.584e-08	2019-09-10 08:30:21 UTC
S190910d	PE_READY ADVOK SKYMAP_READY EMBRIGHT_READY PASTRO_READY DQOK GCN_PRELIM_SENT	1252113996.241211	1252113997.242676	1252113998.264918	3.717e-09	2019-09-10 01:26:35 UTC
S190901ap	PE_READY ADVOK SKYMAP_READY EMBRIGHT_READY PASTRO_READY DQOK GCN_PRELIM_SENT	1251415878.837767	1251415879.837767	1251415880.838844	7.027e-09	2019-09-01 23:31:24 UTC
S190829u	PE_READY ADVNO SKYMAP_READY EMBRIGHT_READY PASTRO_READY DQOK GCN_PRELIM_SENT	1251147973.281494	1251147974.283940	1251147975.283940	5.151e-09	2019-08-29 21:06:19 UTC
S190828l	PE_READY ADVOK SKYMAP_READY EMBRIGHT_READY PASTRO_READY DQOK GCN_PRELIM_SENT	1251010526.884921	1251010527.886557	1251010528.913573	4.629e-11	2019-08-28 06:55:26 UTC
S190828j	PE_READY ADVOK SKYMAP_READY EMBRIGHT_READY PASTRO_READY DQOK GCN_PRELIM_SENT	1251009262.739486	1251009263.756472	1251009264.796332	8.474e-22	2019-08-28 06:34:21 UTC
S190822c	ADVNO SKYMAP_READY EMBRIGHT_READY PASTRO_READY DQOK GCN_PRELIM_SENT	1250472616.589125	1250472617.589203	1250472618.589203	6.145e-18	2019-08-22 01:30:23 UTC
S190816i	PE_READY ADVNO SKYMAP_READY EMBRIGHT_READY PASTRO_READY DQOK GCN_PRELIM_SENT	1249995888.757789	1249995889.757789	1249995890.757789	1.436e-08	2019-08-16 13:05:12 UTC
S190814bv	PE_READY ADVOK SKYMAP_READY EMBRIGHT_READY PASTRO_READY DQOK GCN_PRELIM_SENT	1249852255.996787	1249852257.012957	1249852258.021731	2.033e-33	2019-08-14 21:11:18 UTC
S190808ae	ADVNO SKYMAP_READY EMBRIGHT_READY PASTRO_READY DQOK GCN_PRELIM_SENT	1249338098.496141	1249338099.496141	1249338100.496141	3.366e-08	2019-08-08 22:21:45 UTC
S190728q	PE_READY ADVOK SKYMAP_READY EMBRIGHT_READY PASTRO_READY DQOK GCN_PRELIM_SENT	1248331527.497344	1248331528.546797	1248331529.706055	2.527e-23	2019-07-28 06:45:27 UTC
S190727h	PE_READY ADVOK SKYMAP_READY EMBRIGHT_READY PASTRO_READY DQOK GCN_PRELIM_SENT	1248242630.976288	1248242631.985887	1248242633.180176	1.378e-10	2019-07-27 06:03:51 UTC
S190720a	PE_READY ADVOK SKYMAP_READY EMBRIGHT_READY PASTRO_READY DQOK GCN_PRELIM_SENT	1247616533.703127	1247616534.704102	1247616535.860840	3.801e-09	2019-07-20 00:08:53 UTC
S190718y	ADVOK SKYMAP_READY EMBRIGHT_READY PASTRO_READY DQOK GCN_PRELIM_SENT	1247495729.067865	1247495730.067865	1247495731.067865	3.648e-08	2019-07-18 14:35:34 UTC
S190707q	PE_READY ADVOK SKYMAP_READY EMBRIGHT_READY PASTRO_READY DQOK GCN_PRELIM_SENT	1246527223.118398	1246527224.181226	1246527225.284180	5.265e-12	2019-07-07 09:33:44 UTC
S190706ai	PE_READY ADVOK SKYMAP_READY EMBRIGHT_READY PASTRO_READY DQOK GCN_PRELIM_SENT	1246487218.321541	1246487219.344727	1246487220.585938	1.901e-09	2019-07-06 22:26:57 UTC
S190701ah	PE_READY ADVOK SKYMAP_READY EMBRIGHT_READY PASTRO_READY DQOK GCN_PRELIM_SENT	1246048403.576563	1246048404.577637	1246048405.814941	1.916e-08	2019-07-01 20:33:24 UTC
S190630ag	PE_READY ADVOK SKYMAP_READY EMBRIGHT_READY PASTRO_READY DQOK GCN_PRELIM_SENT	1245955942.175325	1245955943.179550	1245955944.183184	1.435e-13	2019-06-30 18:52:28 UTC
S190602aq	PE_READY ADVOK SKYMAP_READY EMBRIGHT_READY PASTRO_READY DQOK GCN_PRELIM_SENT	1243533584.081266	1243533585.089355	1243533586.346191	1.901e-09	2019-06-02 17:59:51 UTC
S190524q	ADVNO SKYMAP_READY EMBRIGHT_READY PASTRO_READY DQOK GCN_PRELIM_SENT	1242708743.678669	1242708744.678669	1242708746.133301	6.971e-09	2019-05-24 04:52:30 UTC
S190521r	PE_READY ADVOK SKYMAP_READY EMBRIGHT_READY PASTRO_READY DQOK GCN_PRELIM_SENT	1242459856.453418	1242459857.460739	1242459858.642090	3.168e-10	2019-05-21 07:44:22 UTC
S190521g	PE_READY ADVOK SKYMAP_READY EMBRIGHT_READY PASTRO_READY DQOK GCN_PRELIM_SENT	1242442966.447266	1242442967.606934	1242442968.888184	3.801e-09	2019-05-21 03:02:49 UTC
S190519bj	PE_READY ADVOK SKYMAP_READY EMBRIGHT_READY PASTRO_READY DQOK GCN_PRELIM_SENT	1242315361.378873	1242315362.655762	1242315363.676270	5.702e-09	2019-05-19 15:36:04 UTC
S190518bb	ADVNO SKYMAP_READY EMBRIGHT_READY PASTRO_READY DQOK GCN_PRELIM_SENT	1242242376.474609	1242242377.474609	1242242380.922655	1.004e-08	2019-05-18 19:19:39 UTC
S190517h	PE_READY ADVOK SKYMAP_READY EMBRIGHT_READY PASTRO_READY DQOK GCN_PRELIM_SENT	1242107478.819517	1242107479.994141	1242107480.994141	2.373e-09	2019-05-17 05:51:23 UTC
S190513bm	PE_READY ADVOK SKYMAP_READY EMBRIGHT_READY PASTRO_READY DQOK GCN_PRELIM_SENT	1241816085.736106	1241816086.869141	1241816087.869141	3.734e-13	2019-05-13 20:54:48 UTC
S190512at	PE_READY ADVOK SKYMAP_READY EMBRIGHT_READY PASTRO_READY DQOK GCN_PRELIM_SENT	1241719651.411441	1241719652.416286	1241719653.518066	1.901e-09	2019-05-12 18:07:42 UTC
S190510g	ADVOK SKYMAP_READY EMBRIGHT_READY PASTRO_READY DQOK GCN_PRELIM_SENT	1241492396.291636	1241492397.291636	1241492398.293185	8.834e-09	2019-05-10 03:00:03 UTC
S190503bf	PE_READY ADVOK SKYMAP_READY EMBRIGHT_READY PASTRO_READY DQOK GCN_PRELIM_SENT	1240944861.288574	1240944862.412598	1240944863.422852	1.636e-09	2019-05-03 18:54:26 UTC
S190426c	PE_READY ADVOK SKYMAP_READY EMBRIGHT_READY PASTRO_READY DQOK GCN_PRELIM_SENT	1240327332.331668	1240327333.348145	1240327334.353516	1.947e-08	2019-04-26 15:22:15 UTC
S190425z	ADVOK SKYMAP_READY EMBRIGHT_READY PASTRO_READY DQOK	1240215502.011549	1240215503.011549	1240215504.018242	4.538e-13	2019-04-25 08:18:26 UTC
S190421ar	PE_READY ADVOK SKYMAP_READY EMBRIGHT_READY PASTRO_READY DQOK GCN_PRELIM_SENT	1239917953.250977	1239917954.409180	1239917955.409180	1.489e-08	2019-04-21 21:39:16 UTC
S190412m	PE_READY ADVOK SKYMAP_READY EMBRIGHT_READY PASTRO_READY DQOK GCN_PRELIM_SENT	1239082261.146717	1239082262.222168	1239082263.229492	1.683e-27	2019-04-12 05:31:03 UTC
S190408an	PE_READY ADVOK SKYMAP_READY EMBRIGHT_READY PASTRO_READY DQOK GCN_PRELIM_SENT	1238782699.268296	1238782700.287958	1238782701.359863	2.811e-18	2019-04-08 18:18:27 UTC
S190405ar	ADVNO SKYMAP_READY EMBRIGHT_READY PASTRO_READY DQOK	1238515307.863646	1238515308.863646	1238515309.863646	2.141e-04	2019-04-05 16:01:56 UTC

The success of GR: Event Horizon Telescope - M87 Pōwehi

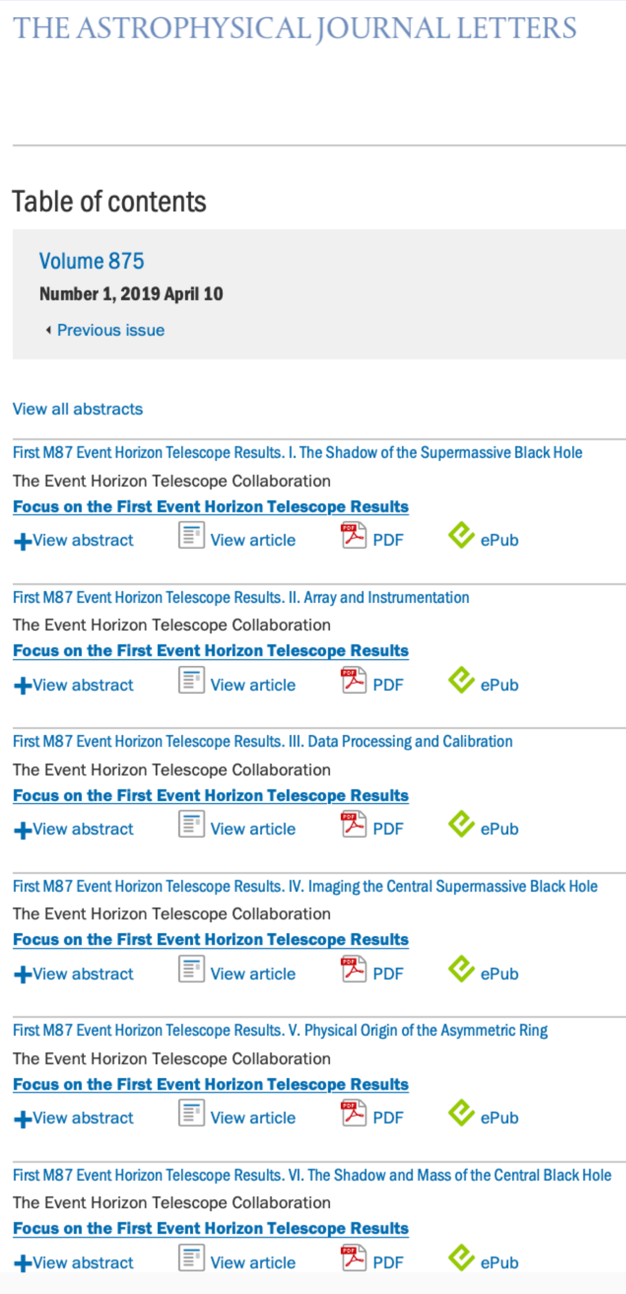

THE ASTROPHYSICAL JOURNAL LETTERS

Table of contents

Volume 875

Number 1, 2019 April 10

‹ Previous issue

View all abstracts

First M87 Event Horizon Telescope Results. I. The Shadow of the Supermassive Black Hole

The Event Horizon Telescope Collaboration

Focus on the First Event Horizon Telescope Results

+View abstract View article PDF ePub

First M87 Event Horizon Telescope Results. II. Array and Instrumentation

The Event Horizon Telescope Collaboration

Focus on the First Event Horizon Telescope Results

+View abstract View article PDF ePub

First M87 Event Horizon Telescope Results. III. Data Processing and Calibration

The Event Horizon Telescope Collaboration

Focus on the First Event Horizon Telescope Results

+View abstract View article PDF ePub

First M87 Event Horizon Telescope Results. IV. Imaging the Central Supermassive Black Hole

The Event Horizon Telescope Collaboration

Focus on the First Event Horizon Telescope Results

+View abstract View article PDF ePub

First M87 Event Horizon Telescope Results. V. Physical Origin of the Asymmetric Ring

The Event Horizon Telescope Collaboration

Focus on the First Event Horizon Telescope Results

+View abstract View article PDF ePub

First M87 Event Horizon Telescope Results. VI. The Shadow and Mass of the Central Black Hole

The Event Horizon Telescope Collaboration

Focus on the First Event Horizon Telescope Results

+View abstract View article PDF ePub

The EHT Collaboration et al.

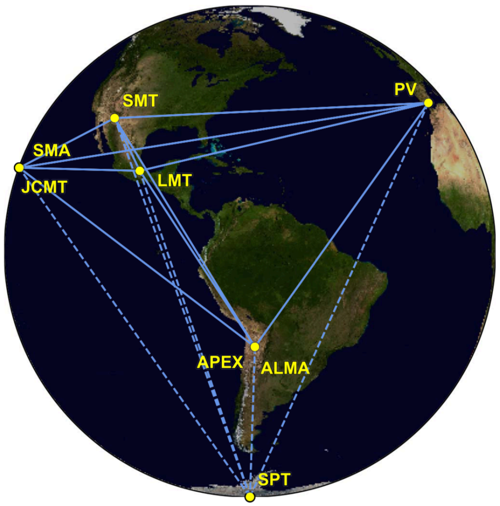

Figure 1. Eight stations of the EHT 2017 campaign over six geographic locations as viewed from the equatorial plane. Solid baselines represent mutual visibility on M87* (+12° declination). The dashed baselines were used for the calibration source 3C279 (see Papers III and IV).

The Universe under the Microscope – Astrophysics at High Angular Resoluti IOP Publishing
Journal of Physics: Conference Series **131** (2008) 012053 doi:10.1088/1742-6596/131/1/012053

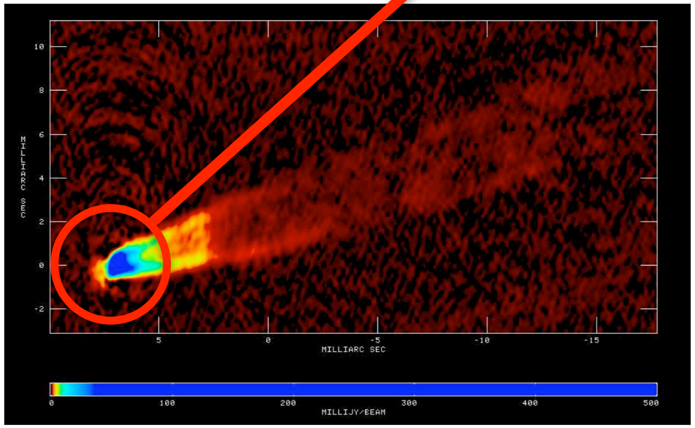

Figure 2. A composite VLBA image of M87 at 43 GHz made by summing the images from the first 9 epochs of the movie project. The resolution is 0.43 × 0.21 mas elongated along position angle −16°. The image peak is 643 mJy beam^{-1} and the off-source rms is 0.18 mJy beam^{-1}. Because this image is the sum of several images made at different times, individual features will be blurred out and the jet will appear smoother than it actually is, much like what is seen in a long-exposure photograph of moving water.

The EHT Collaboration et al.

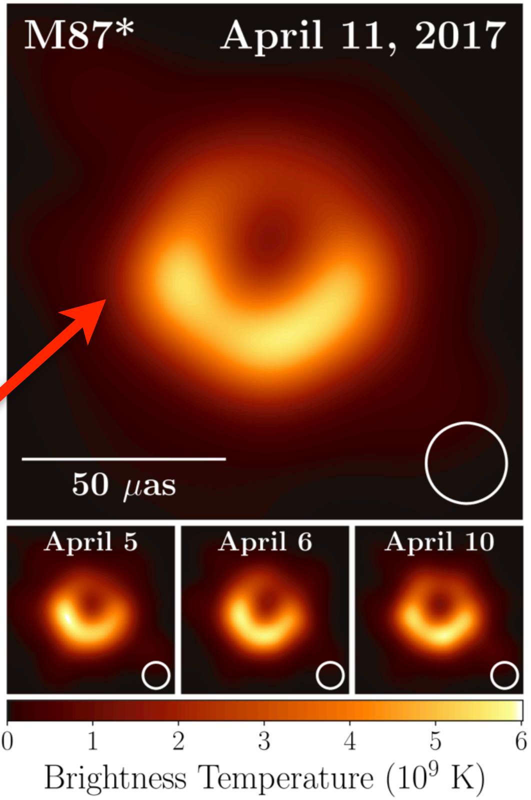

Figure 3. Top: EHT image of M87* from observations on 2017 April 11 as a representative example of the images collected in the 2017 campaign. The image is the average of three different imaging methods after convolving each with a circular Gaussian kernel to give matched resolutions. The largest of the three kernels (20 μas FWHM) is shown in the lower right. The image is shown in units of brightness temperature, $T_b = S\lambda^2/2k_B\Omega$, where S is the flux density, λ is the observing wavelength, k_B is the Boltzmann constant, and Ω is the solid angle of the resolution element. Bottom: similar images taken over different days showing the stability of the basic image structure and the equivalence among different days. North is up and east is to the left.

https://iopscience.iop.org/article/10.1088/1742-6596/131/1/012053/pdf?fbclid=IwAR258WA8ofbOCkeFwO3HuaD9yZQ0V4FNE9MGCsmj1r_y229EuuqgtJnbNuI

What is the problem with GR then?

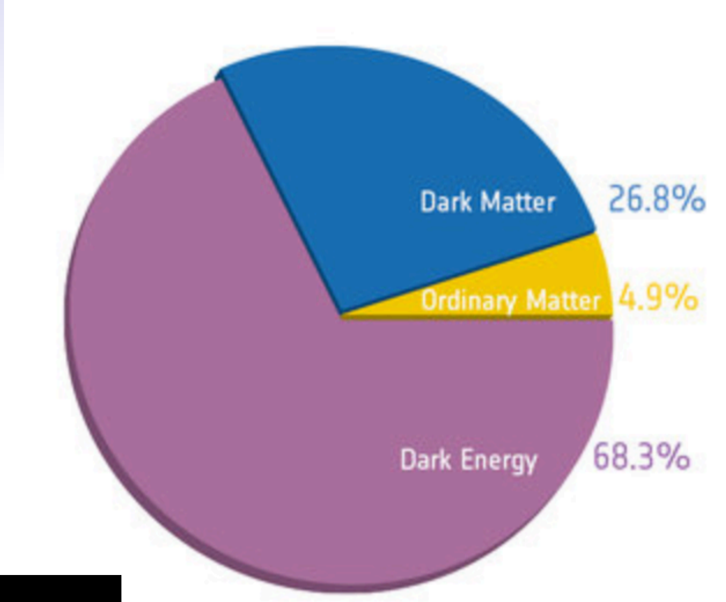

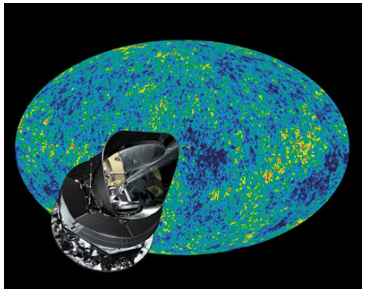

After Planck

No dark matter detected:

2000 - MACHO (microlensing)
2014, 2016 - WIMP particles (LUX, PandaX-II, Xenon100)
2015 - Axions (Axion Dark Matter Experiment, Centre for Experimental Nuclear Physics and Astrophysics (CENPA), University of Washington)
2016 - Sterile neutrinos (IceCube)
2016 - Extra dimensions (LHC)
2016 - Supersymmetric particles (LHC)
2019 - stau, Higgsino not found (ATLAS, LHC)

Dark energy: Cosmological constant?

But this vacuum energy density is 60 orders of magnitude smaller than the theoretical prediction of zero-point energy in quantum field theory

Quantum gravity: several attempts, no established final theory

Its low energy (infrared) limit should give GR and corrections at first order —> effective field theory (EFT)

→ Both DM and DE interact only gravitationally

→ Hope to test EFT in the near future

→ Need for modifying GR !

What else is the problem with GR?

4) Highly non-renormalizable,

can not be formulated as a QFT as for the other fundamental forces,
can not directly be embedded into the standard model of particle physics

5) Early universe inflation requires additional field (s),

best fit with CMB data given by Einstein gravity with an inflaton field (slow-roll model with a concave potential)

Y. Akrami *et al.* [Planck Collaboration], “Planck 2018 results. X. Constraints on inflation,” arXiv:1807.06211 [astro-ph.CO].

6) Tensions in the determination of the Hubble-parameter

CMB measurements from Planck:

67.74 ± 0.46 km/s/Mpc

SNIa measurements from SHoES21:

73.24 ± 1.74 km/s/Mpc

GW170817 luminosity distance and optical transient:

$70.0^{+12.0}_{-8.0}$ km/s/Mpc

nature Accelerated Article Preview

LETTER
doi:10.1038/nature24471

A gravitational-wave standard siren measurement of the Hubble constant

The LIGO Scientific Collaboration and The Virgo Collaboration*, The 1M2H Collaboration*, The Dark Energy Camera GW-EM Collaboration and the DES Collaboration*, The DLT40 Collaboration*, The Las Cumbres Observatory Collaboration*, The VINROUGE Collaboration* & The MASTER Collaboration*

RESEARCH LETTER

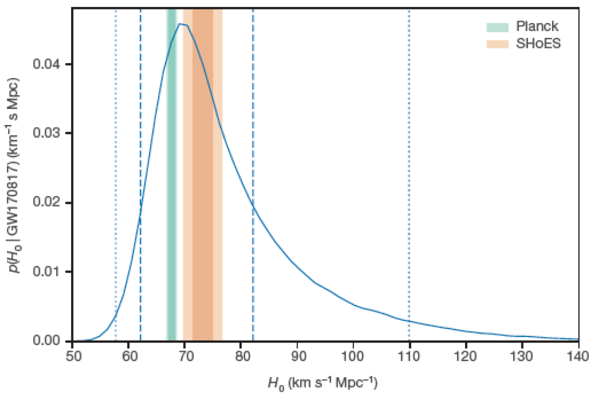

Figure 1 | GW170817 measurement of H_0. The marginalized posterior density for H_0, $p(H_0 \mid \mathrm{GW170817})$, is shown by the blue curve. Constraints at 1σ (darker shading) and 2σ (lighter shading) from Planck[20] and SHoES[21] are shown in green and orange, respectively. The maximum a posteriori value and minimal 68.3% credible interval from this posterior density function is $H_0 = 70.0^{+12.0}_{-8.0}$ km s^{-1} Mpc^{-1}. The 68.3% (1σ) and 95.4% (2σ) minimal credible intervals are indicated by dashed and dotted lines, respectively.

7) Problems in defining gravitational energy-momentum, null boundary terms in the action, occurrence of singularities…

How to go beyond GR?

- By relaxing one of the fundamental hypotheses of the Lovelock theorem that makes Einstein theory unique:

- invariance under diffeomorphisms,

  (ex: Lorentz-invariance breaking, massive gravity)

- locality,

- pure metric formulation in four space-time dimensions

  (add new fields, representing gravity, ex: scalar-tensor theories)

- In general they contain one or more extra d.o.f-s, used to

- describe dark energy (fifth force)

- make the theory renormalizable (cure the UV problem of GR)

- Requirements:

- compatibility with observations (Solar System, etc...)

- stability → perturbations

this talk

Various techniques for discussing perturbations

A) Newman-Penrose formalism (1+1+1+1 decomposition)

pros: first order diff. eqs,

cons: myriad of variables, 4 types of non-commuting derivatives

- ex: black hole perturbations (Chandrasekhar): 70 coupled diff. eqs. for 50 indep. vars.
- ex: vacuum Kerr-Schild space-times (my PhD thesis)

B) 2+1+1 decomposition based on kinematic quantities (optical scalars) + electric and magnetic projections of the Weyl tensor

pros: generically applicable

cons: still many variables

C) metric perturbations

pros: only 10 metric functions

cons: requires full gauge fixing

versions:

3+1 decomposition, ADM variables

2+1+1 decomposition, orthogonal double foliation

L.Á. Gergely, Z. Kovács, Phys. Rev. D 72, 064015 (2005)
Z. Kovács, L.Á. Gergely, Phys. Rev. D 77, 024003 (2008)

2+1+1 decomposition, nonorthogonal double foliation

C. Gergely, Z. Keresztes, L. Á. Gergely, Universe 4, 9 (2018)
C. Gergely, Z. Keresztes, L. Á. Gergely, Phys. Rev. D 99, 124019 (2019)

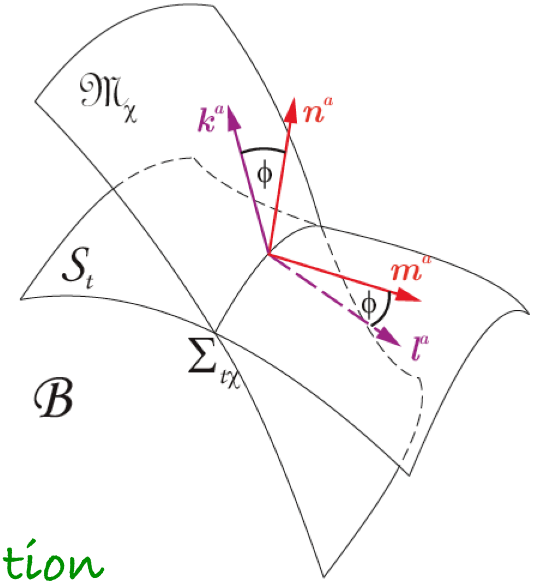

2+1+1 decomposition, orthogonal double foliation

L.Á. Gergely, Z. Kovács, Phys. Rev. D 72, 064015 (2005)
Z. Kovács, L.Á. Gergely, Phys. Rev. D 77, 024003 (2008)

two 3D hypersurfaces: $\mathcal{S}_t$ (constant time parameter: t)

$\mathcal{M}_\chi$ (constant spatial parameter: χ)

intersection 2D surface: $\Sigma_{t\chi}$ with **induced metric**: h_{ab}

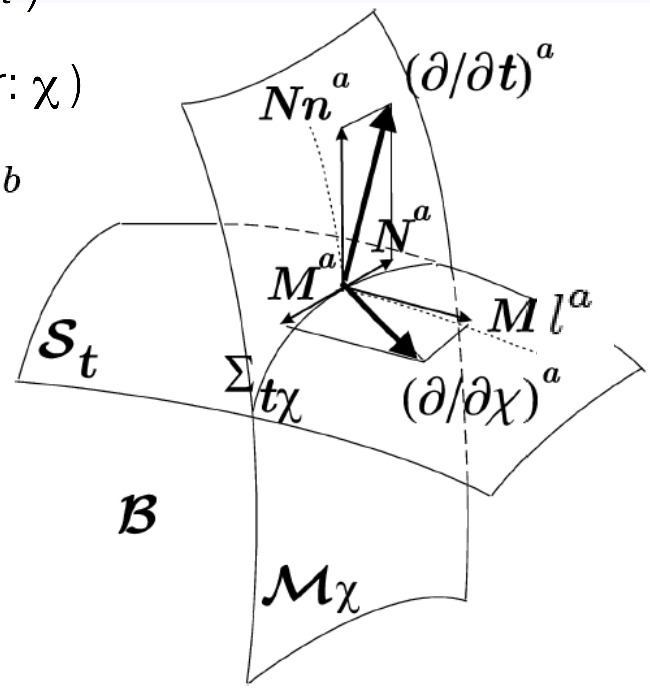

2+1+1 decomposition of 4D metric:

$$\tilde{g}_{ab} = h_{ab} - n_a n_b + l_a l_b$$

evolution vectors:

$$\begin{aligned} \left(\frac{\partial}{\partial t}\right)^a &= Nn^a + N^a \qquad & n^a n_a &= -1 \\ \left(\frac{\partial}{\partial \chi}\right)^a &= Ml^a + M^a \qquad & l^a l_a &= 1 \end{aligned}$$

due to co-dimensions 2, the embedding of $\Sigma_{t\chi}$ is complicated:

extrinsic curvatures:	$K_{ab} = h^c_a h^d_b \tilde{\nabla}_c n_d$	$L_{ab} = h^c_a h^d_b \tilde{\nabla}_c l_d$
normal fundamental forms:	$\mathcal{K}_a = h^c_a l^d \tilde{\nabla}_c n_d$	$\mathcal{L}_a = -h^c_a n^d \tilde{\nabla}_d l_c = \mathcal{K}_a$
normal fundamental scalars:	$\mathcal{K} = l^d l^c \tilde{\nabla}_c n_d$	$\mathcal{L} = n^d n^c \tilde{\nabla}_c l_d$
accelerations:	$\mathfrak{a}_a = h^d_a n^c \tilde{\nabla}_c n_d$	$\mathfrak{b}_a = h^d_a l^c \tilde{\nabla}_c l_d$

Gravitational dynamics with orthogonal double foliations

4D **line-element** in ADM-like variables (adapted to the 2+1+1 decomposition):

$$ds^2 = \begin{pmatrix} dt & d\chi & dy^a \end{pmatrix} \begin{pmatrix} -N^2 + N_c N^c & N_c M^c & N_b \\ N_c M^c & M^2 + M_c M^c & M_b \\ N_a & M_a & h_{ab} \end{pmatrix} \begin{pmatrix} dt \\ d\chi \\ dy^b \end{pmatrix}$$

gravitational variables: $\{h_{ab}, M^a, M\}$ (3+2+1 = 6 metric variables)

generalised velocities: $\{K_{ab}, \mathcal{K}^a, \mathcal{K}\}$

(extrinsic curvature, normal fundamental form, normal fundamental scalar)

non-dynamical metric variables: $\{N, N^a\}$ (1+2 = 3 metric variables)

(lapse, shift: – Lagrange-multipliers in the action

– coordinate system choice / diffeomorphism / gauge freedom)

→ only **9 metric variables**

one of the gauge degrees of freedom was consumed by orthogonality!

This a problem, it hampers unambiguous gauge fixing!

Nonorthogonal foliations

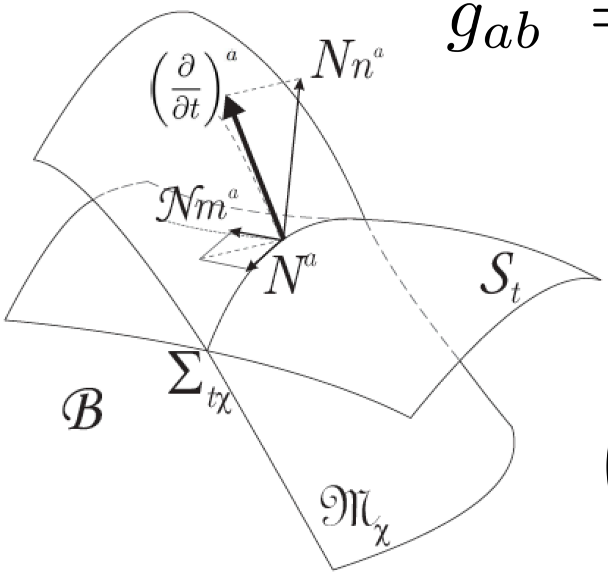

$$\tilde{g}_{ab} = -n_a n_b + m_a m_b + g_{ab}$$

from the duality relations:

$$\left(\frac{\partial}{\partial t}\right)^a = Nn^a + N^a + \boxed{\mathcal{N}m^a}$$

$$\left(\frac{\partial}{\partial \chi}\right)^a = Mm^a + M^a$$

the 10th metric variable!

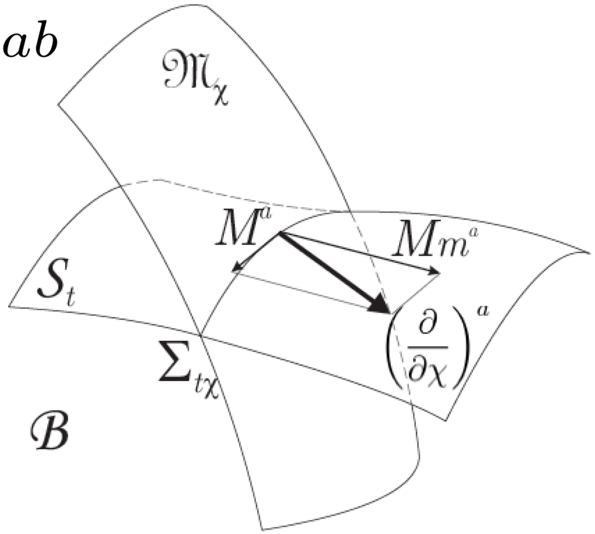

Lie-brackets

n^a vorticity-free, orthogonal to S_t (Frobenius-theorem)

	$[n,m]^a$	$[n,F_\mathbf{j}]^a$	$[m,F_\mathbf{j}]^a$
n^a	$\frac{1}{M}\left[\partial_\chi(\ln N) - \frac{1}{M}M^\mathbf{j}\partial_\mathbf{j}(\ln N)\right]$	$\partial_\mathbf{j}(\ln N)$	$\boxed{0}$
m^a	$\frac{1}{MN}\left[-\partial_t M + \underline{\partial_\chi \mathcal{N}} + N^\mathbf{j}\partial_\mathbf{j} M \underline{- M^\mathbf{j}\partial_\mathbf{j}\mathcal{N}}\right]$	$\boxed{\frac{M}{N}\partial_\mathbf{j}\left(\frac{\mathcal{N}}{M}\right)}$	$\partial_\mathbf{j}(\ln M)$
$F_\mathbf{i}^a$	$\frac{1}{MN}\left(-\partial_t M^\mathbf{i} + \partial_\chi N^\mathbf{i} + N^\mathbf{j}\partial_\mathbf{j} M^\mathbf{i} - M^\mathbf{j}\partial_\mathbf{j} N^\mathbf{i}\right)$	$\frac{1}{N}\left[\partial_\mathbf{j} N^\mathbf{i} \underline{- \frac{\mathcal{N}}{M}\partial_\mathbf{j} M^\mathbf{i}}\right]$	$\frac{\partial_\mathbf{j} M^\mathbf{i}}{M}$

m^a has vorticity

The geometrical quantities of normals

Decomposition of the **covariant derivatives:**

$$
\begin{aligned}
\tilde{\nabla}_a n_b &= K_{ab} + 2m_{(a}\mathcal{K}_{b)} + m_a m_b \mathcal{K} - n_a \mathfrak{a}_b + n_a m_b \mathcal{L}^* \\
\tilde{\nabla}_a l_b &= L_{ab} + 2k_{(a}\mathcal{L}_{b)} + k_a k_b \mathcal{L} + l_a \mathfrak{b}_b + l_a k_b \mathcal{K}^* \\
\tilde{\nabla}_a m_b &= K^*_{ab} + l_a \mathcal{K}^*_b + l_b \mathcal{L}_a + l_a l_b \mathcal{K}^* - k_a \left(\mathfrak{a}^*_b - l_b \mathcal{L}\right) \\
\tilde{\nabla}_a k_b &= L^*_{ab} + n_a \mathcal{L}^*_b + n_b \mathcal{K}_a + n_a n_b \mathcal{L}^* + m_a \left(\mathfrak{b}^*_b + n_b \mathcal{K}\right)
\end{aligned}
$$

Geometrical quantities involved:

$K_{ab} = g^c_a g^d_b \tilde{\nabla}_c n_d$	$L_{ab} = g^c_a g^d_b \tilde{\nabla}_c l_d$
$\mathcal{K}_a = g^c_a m^d \tilde{\nabla}_c n_d$	$\mathcal{L}_a = -g^c_a k^d \tilde{\nabla}_c l_d$
$\mathcal{K} = m^d m^c \tilde{\nabla}_c n_d$	$\mathcal{L} = k^d k^c \tilde{\nabla}_c l_d$
$\mathfrak{a}_a = g^d_a n^c \tilde{\nabla}_c n_d$	$\mathfrak{b}_a = g^d_a l^c \tilde{\nabla}_c l_d$

$K^*_{ab} = g^c_a g^d_b \tilde{\nabla}_c k_d$	$L^*_{ab} = g^c_a g^d_b \tilde{\nabla}_c m_d$
$\mathcal{K}^*_a = g^d_a l^c \tilde{\nabla}_c k_d$	$\mathcal{L}^*_a = -g^d_a n^c \tilde{\nabla}_c m_d$
$\mathcal{K}^* = l^d l^c \tilde{\nabla}_c k_d$	$\mathcal{L}^* = n^c n^d \tilde{\nabla}_c m_d$
$\mathfrak{a}^*_a = g^d_a k^c \tilde{\nabla}_c k_d$	$\mathfrak{b}^*_a = g^d_a m^c \tilde{\nabla}_c m_d$

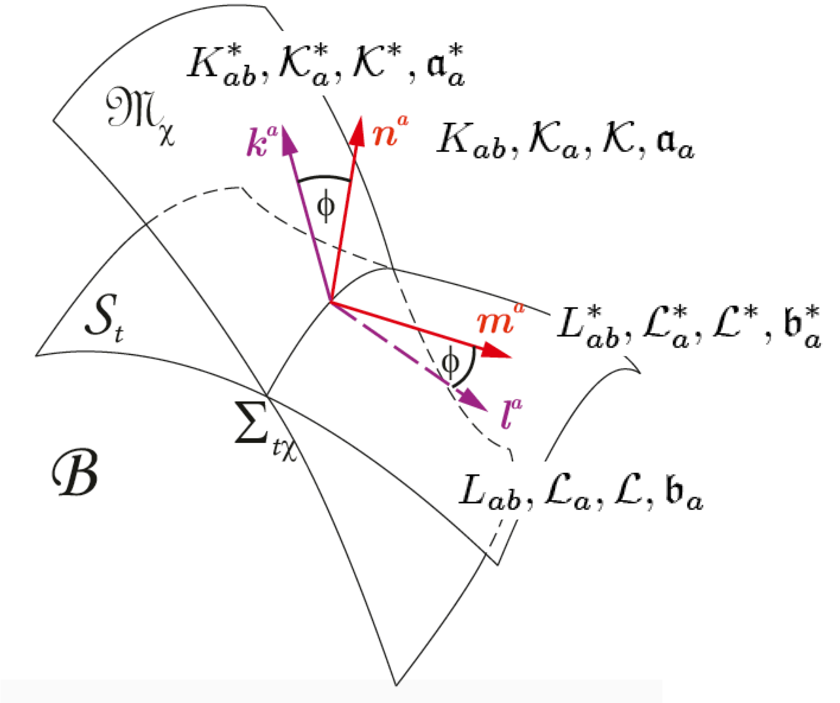

The 10th metric variable gives vorticity to the basis vectors & is related to the Lorentz-rotation of the bases

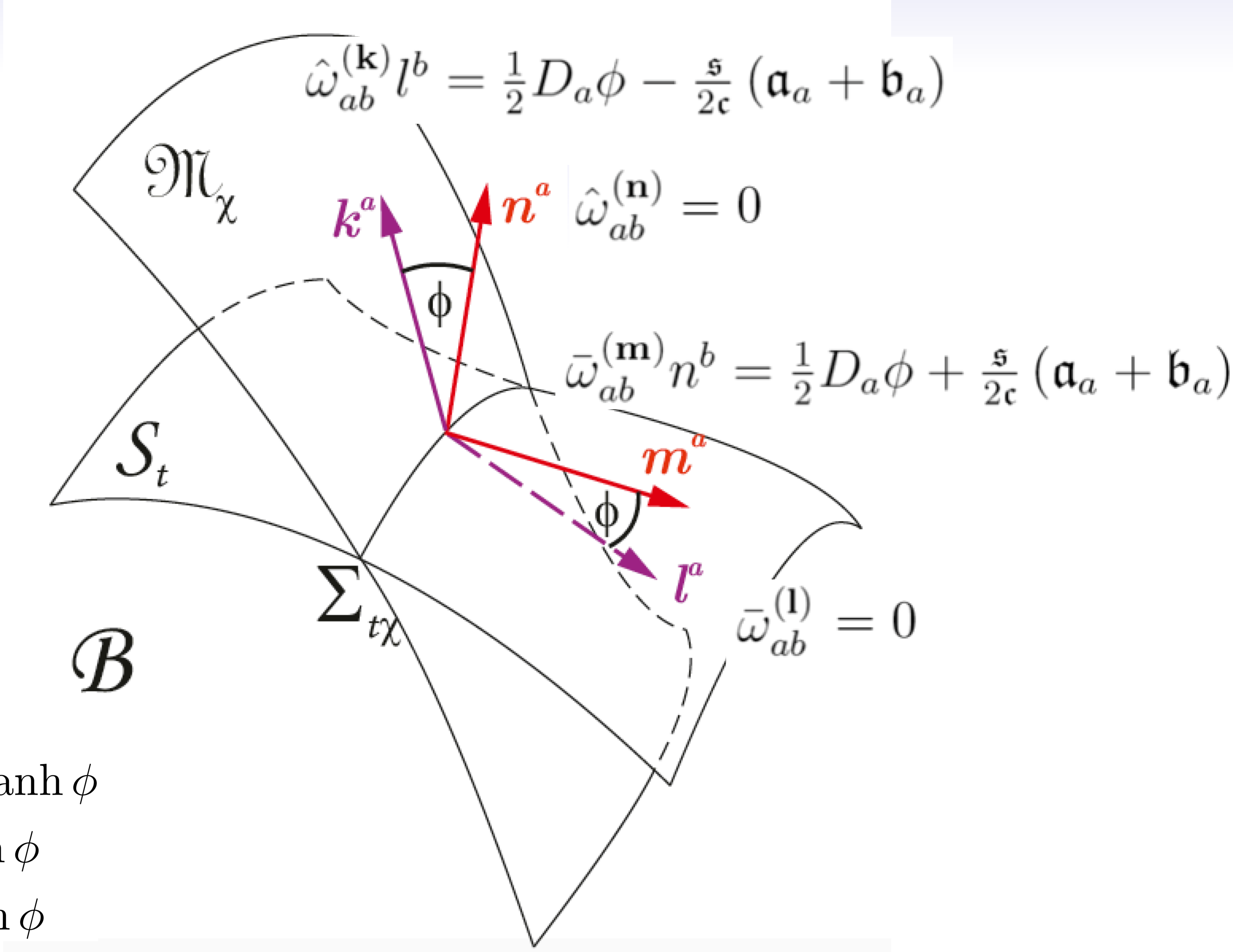

$$\hat{\omega}^{(\mathbf{k})}_{ab} l^b = \tfrac{1}{2} D_a\phi - \tfrac{\mathfrak{s}}{2\mathfrak{c}}\left(\mathfrak{a}_a + \mathfrak{b}_a\right)$$

$$\hat{\omega}^{(\mathbf{n})}_{ab} = 0$$

$$\bar{\omega}^{(\mathbf{m})}_{ab} n^b = \tfrac{1}{2} D_a\phi + \tfrac{\mathfrak{s}}{2\mathfrak{c}}\left(\mathfrak{a}_a + \mathfrak{b}_a\right)$$

$$\bar{\omega}^{(\mathbf{l})}_{ab} = 0$$

$$\begin{aligned}\mathcal{N} &= N \tanh\phi \\ \mathfrak{s} &= \sinh\phi \\ \mathfrak{c} &= \cosh\phi\end{aligned}$$

The velocity phase space

Generalised coordinates: $\{g_{ab}, M^a, M\}$

Generalised velocities: $\{K_{ab}, \mathcal{K}^a, \mathcal{K}\}$

$$K_{ab} = \frac{1}{N}\left[\underline{\frac{1}{2}\partial_t g_{ab}} - D_{(a}N_{b)}\right] - \frac{\mathfrak{s}}{M\mathfrak{c}}\left[\frac{1}{2}\partial_\chi g_{ab} - D_{(a}M_{b)}\right]$$

$$\mathcal{K}^a = \frac{1}{2MN}\left(\underline{\partial_t M^a} - \partial_\chi N^a - N^b D_b M^a + M^b D_b N^a\right) - \frac{M}{2N}D^a\left(\frac{\mathcal{N}}{M}\right)$$

$$\mathcal{K} = \frac{1}{MN}\left[\underline{\partial_t M} - \partial_\chi \mathcal{N} - N^a D_a M + M^a D_a \mathcal{N}\right]$$

$\uparrow$

time derivatives!

Variables expressing gauge freedom: $N,\ \ N^a, \boxed{\mathcal{N}}$

Non-dynamical geometrical quantities: $\boxed{L^*_{ab}\ ,\ \mathcal{L}^*}$

$$L^*_{ab} = \frac{1}{M}\left[\frac{1}{2}\partial_\chi g_{ab} - D_{(a}M_{b)}\right]$$

$$\mathcal{L}^* = -\frac{1}{M}\left[\partial_\chi\left(\ln N\right) - M^a D_a\left(\ln N\right)\right]$$

2+1+1 form of the gravitational action in GR

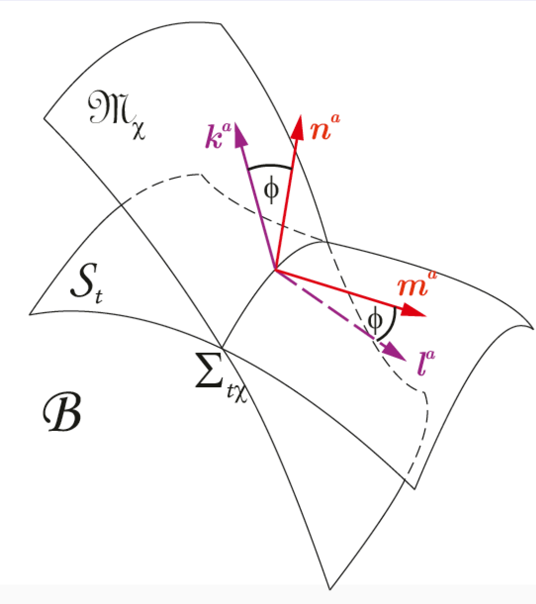

Gauss identity:

($\Sigma_{t\chi}$ projection of the Riemann-tensor in the n^a,m^a basis):

$$R_{abcd} = g^i_a g^l_b g^k_c g^l_d \tilde{R}_{ijkl} + 2\left(L^*_{a[c} L^*_{d]b} - K_{a[c} K_{d]b}\right)$$

Einstein-Hilbert action: $S_{EH} = \int d^4x \sqrt{-\tilde{g}}\tilde{R}$

2+1+1 decomposition of the **metric determinant:** $\sqrt{-\tilde{g}} = NM\sqrt{g}$

2+1+1 decomposition of the **curvature scalar** (twice contracted Gauss-identity):

$$\begin{aligned}\tilde{R} \quad = \quad & R + K^2 + K_{ab}K^{ab} + 2\mathcal{K}^b\mathcal{K}_b + 2\mathcal{K}\left(K - \mathcal{K}\right) + 2\tilde{\mathfrak{L}}_{\mathbf{n}}\left(K + \mathcal{K}\right) \\ & - \left(L^*\right)^2 - L^*_{ab}L^{*ab} - 2\mathcal{L}^*\left(\mathcal{L}^* - L^*\right) - 2\tilde{\mathfrak{L}}_{\mathbf{m}}\left(L^* - \mathcal{L}^*\right) \\ & -2\left[\frac{D_aD^aN}{N} + \frac{D_aD^aM}{M} + \frac{D^aMD_aN}{NM}\right]\end{aligned}$$

D-derivatives

χ-derivatives

R+time-derivatives

Legendre transformation

Lagrangian density: $\mathcal{L}^G = \pi^{ab}\dot{g}_{ab} + p_a\dot{M}^a + p\dot{M} - \mathcal{H}^G + \mathcal{L}^G_t + \mathcal{L}^G_\chi + \mathcal{L}^G_D$

Boundary terms: $\mathcal{L}^G_t = 2\partial_t\left[\sqrt{g}M\left(K + \mathcal{K}\right)\right]$

$$\mathcal{L}^G_\chi = 2\partial_\chi\left[\sqrt{g}\left(N\mathcal{L}^* - N_a\mathcal{K}^a \underline{- \mathcal{N}\mathcal{K})}\right]\right.$$

$$\mathcal{L}^G_D = -2\sqrt{g}D_a\left[MD^aN + NM^a\mathcal{L}^* + N^b\left(MK^a{}_b - M^a\mathcal{K}_b\right)\right.$$
$$\left.\underline{+\mathcal{N}\left(M\mathcal{K}^a - M^a\mathcal{K}\right)}\right]$$

Hamiltonian density: $\mathcal{H}^G = N\mathcal{H}^G_\perp + N^a\mathcal{H}^G_a + \underline{\mathcal{N}\mathcal{H}^G_\mathcal{N}}$

new

Hamiltonian and momentum constraints:

$$\mathcal{H}^G_\perp = \sqrt{g}\left\{-M\left(R + 3L^{*ab}L^*_{ab} - L^{*2}\right) + 2g^{ab}\left(\partial_\chi - \mathfrak{L}_\mathbf{M}\right)L^*_{ab}\right.$$
$$\left.+2D^aD_aM + M\left[K_{ab}K^{ab} + 2\mathcal{K}_a\mathcal{K}^a - K^2 - 2K\mathcal{K}\right]\right\}$$

$$\mathcal{H}^G_a = -2\sqrt{g}\left\{D_b\left[K^b{}_aM - Mg^b{}_a\left(K + \mathcal{K}\right)\right] + \left(\partial_\chi - \mathfrak{L}_\mathbf{M}\right)\mathcal{K}_a\right.$$
$$\left.+\mathcal{K}_aML^* + KD_aM\right\}$$

new

$$\mathcal{H}^G_\mathcal{N} = -2\sqrt{g}\left\{M\left[L^*\mathcal{K} - L^*_{ab}K^{ab}\right] - \left(\partial_\chi - \mathfrak{L}_\mathbf{M}\right)K\right.$$
$$\left.+\frac{1}{M}D_a\left(M^2\mathcal{K}^a\right)\right\}$$

Hamiltonian dynamics

Generalised momenta expressed with generalised velocities $\{K_{ab}, \mathcal{K}^a, \mathcal{K}\}$:

$$\pi^{ab} = M\sqrt{g}\left[K^{ab} - g^{ab}\left(K + \mathcal{K}\right)\right]$$

$$p^a = 2\sqrt{g}\mathcal{K}^a$$

$$p = -2\sqrt{g}\mathcal{K}$$

Boundary terms: (in terms of momenta)

$$\mathcal{L}_t^G = -\partial_t\left(\pi + \frac{Mp}{2}\right)$$

$$\mathcal{L}_\chi^G = \partial_\chi\left[2\sqrt{g}N\mathcal{L}^* - N_a p^a \underline{+ \mathcal{N}\left(\frac{\pi}{M} - \frac{p}{2}\right)}\right]$$

$$\mathcal{L}_D^G = -D_a\left\{2\sqrt{g}\left(MD^aN + NM^a\mathcal{L}^*\right) + N^b\left[2\pi^a{}_b - \left(\pi + \frac{Mp}{2}\right)g^a{}_b - M^a p_b\right]\right.$$
$$\left.\underline{+\mathcal{N}\left[Mp^a + M^a\left(\frac{\pi}{M} - \frac{p}{2}\right)\right]}\right\}$$

Hamiltonian and momentum constraints (in terms of momenta):

$$\mathcal{H}_\perp^G = \sqrt{g}\left[-M\left(R + 3L^{*ab}L^*_{ab} - L^{*2}\right) + 2g^{ab}\left(\partial_\chi - \mathfrak{L}_{\mathbf{M}}\right)L^*_{ab} + 2D^aD_aM\right]$$
$$+ \frac{M}{\sqrt{g}}\left[\frac{1}{M^2}\left(\pi_{ab}\pi^{ab} - \frac{\pi^2}{2}\right) + \frac{1}{2}p_ap^a + \frac{1}{8}p^2 - \frac{\pi p}{2M}\right]$$

$$\mathcal{H}_a^G = -2D_b\pi^b_a + pD_aM - \left(\partial_\chi - \mathfrak{L}_{\mathbf{M}}\right)p_a$$

$$\underline{\mathcal{H}_\mathcal{N}^G = 2L^*_{ab}\pi^{ab} - 2p^aD_aM - MD_ap^a - \left(\partial_\chi - \mathfrak{L}_{\mathbf{M}}\right)p}$$

← **new**

Poisson brackets

Poisson brackets of two functionals:

$$\{f(\chi,y),h(\chi',y')\}=\int d\chi''\int dy''\left(\frac{\delta f(\chi,y)}{\delta g^C(\chi'',y'')}\frac{\delta h(\chi',y')}{\delta\pi_C(\chi'',y'')}-\frac{\delta f(\chi,y)}{\delta\pi_C(\chi'',y'')}\frac{\delta h(\chi',y')}{\delta g^C(\chi'',y'')}\right)$$

with:

$$\begin{aligned} f(\chi,y) &\equiv f\left(\chi,y;g^A(\chi,y),\pi_B(\chi,y)\right)\\ h(\chi,y) &\equiv h\left(\chi,y;g^A(\chi,y),\pi_B(\chi,y)\right)\\ y &\equiv \{y^1,y^2\}\end{aligned}$$

$$\begin{aligned} g^A &\equiv \{g_{ab},M^a,M\}\\ \pi_A &\equiv \{\pi^{ab},p_a,p\}\end{aligned}$$

Poisson brackets of canonical pairs: $\{g^A(\chi,y),\pi_B(\chi',y')\} \;=\; \delta^A_B\delta(\chi-\chi')\delta(y-y')$

Smeared Hamiltonian density:

$$\begin{aligned} \mathcal{H}^G[N,N^a,\mathcal{N}] &= \mathcal{H}^G_\perp[N]+\mathcal{H}^G_a[N^a]+\underline{\mathcal{H}^G_{\mathcal{N}}[\mathcal{N}]}\\ \mathcal{H}^G_\perp[N] &= \int d\chi\int dy N(\chi,y)\mathcal{H}^G_\perp(\chi,y)\\ \mathcal{H}^G_a[N^a] &= \int d\chi\int dy N^a(\chi,y)\mathcal{H}^G_a(\chi,y)\\ \underline{\mathcal{H}^G_{\mathcal{N}}[\mathcal{N}]} &\underline{= \int d\chi\int dy \mathcal{N}(\chi,y)\mathcal{H}^G_{\mathcal{N}}(\chi,y)}\end{aligned}$$

new

Canonical equations:

$$\begin{aligned} \dot g^A &\equiv \{g^A(\chi,y),\mathcal{H}^G\}=\frac{\delta\mathcal{H}^G[N,N^a,\mathcal{N}]}{\delta\pi_A(\chi,y)}\;,\\ \dot\pi_A &\equiv \{\pi_A(\chi,y),\mathcal{H}^G\}=-\frac{\delta\mathcal{H}^G[N,N^a,\mathcal{N}]}{\delta g^A(\chi,y)}\end{aligned}$$

Explicit form of canonical equations

Canonical coordinate evolutions:

$$\dot{g}_{cd} = \frac{\delta \mathcal{H}^G\left[N, N^a, \mathcal{N}\right]}{\delta \pi^{cd}\left(\chi, y\right)} = \frac{N}{\sqrt{g}}\left[\frac{1}{M}\left(2\pi_{cd} - g_{cd}\pi\right) - \frac{1}{2} g_{cd} p\right] + 2D_{(c}N_{d)} + \underline{2\mathcal{N} L^*_{cd}}$$

$$\dot{M}^c = \frac{\delta \mathcal{H}^G\left[N, N^a, \mathcal{N}\right]}{\delta p_c\left(\chi, y\right)} = N\frac{M}{\sqrt{g}} p^c + \left(\partial_\chi - \mathfrak{L}_{\mathbf{M}}\right) N^c \underline{- \mathcal{N} D^c M + M D^c \mathcal{N}}$$

$$\dot{M} = \frac{\delta \mathcal{H}^G\left[N, N^a, \mathcal{N}\right]}{\delta p\left(\chi, y\right)} = \frac{N}{2\sqrt{g}}\left(\frac{1}{2} M p - \pi\right) + \mathfrak{L}_{\mathbf{N}} M + \underline{\left(\partial_\chi - \mathfrak{L}_{\mathbf{M}}\right) \mathcal{N}}$$

new

Canonical momenta evolutions:

$$\dot{\pi}^{cd} = -\frac{\delta \mathcal{H}^G\left[N\right]}{\delta g_{cd}\left(\chi, y\right)} = \text{known terms with } \left(N,\ N^a\right) + \underline{\text{new terms with } \mathcal{N}}$$

$$\dot{p}_c = -\frac{\delta \mathcal{H}^G\left[N\right]}{\delta M^c\left(\chi, y\right)} = \text{known terms with } \left(N,\ N^a\right) + \underline{\text{new terms with } \mathcal{N}}$$

$$\dot{p} = -\frac{\delta \mathcal{H}^G\left[N\right]}{\delta M\left(\chi, y\right)} = \text{known terms with } \left(N,\ N^a\right) + \underline{\text{new terms with } \mathcal{N}}$$

Gravitational scalar-tensor theories

Horndeski-theory: the most general scalar-tensor theory with at most second order dynamics for both the scalar and the metric

G.W. Horndeski, Int. J. Theor. Phys. 10, 363 (1974)
C. Deffayet, G. Esposito-Farese, A. Vikman, Phys. Rev. D 79, 084003 (2009)
C. Deffayet, S. Deser, G. Esposito-Farese, Phys. Rev. D 80, 064015 (2009)

Includes: GR, quintessence, k-essence, Brans-Dicke, f(R), galileon …

The effective field theory (EFT) approach: action depending of geometric scalars, second order dynamics, space derivatives could be of higher order: GLPV theories / beyond Horndeski theories

J. Gleyzes, D. Langlois, F. Piazza, F. Vernizzi, J. Cosmos. Astropart. Phys. 08 (2013) 025.

Kinetic braiding subclass of Horndeski and beyond Horndeski theories:

$$
\begin{aligned}
L_{c=1}^{EFT} &= G_2\left(X,\phi\right)+G_3\left(X,\phi\right)\Box\phi+B_4\left(X,\phi\right)\tilde{R} \\
&\quad -\frac{4}{X}B_{4,X}\left(X,\phi\right)\left(\phi^a\phi^b\phi_{ab}\Box\phi-\phi^a\phi_{ab}\phi_c\phi^{cb}\right)
\end{aligned}
$$

$$
\begin{aligned}
X &= \tilde{g}^{ab}\partial_a\phi\partial_b\phi\ , \\
\phi_a &= \tilde{\nabla}_a\phi=\partial_a\phi\ , \\
\phi_{ab} &= \tilde{\nabla}_a\tilde{\nabla}_b\phi\ , \\
\Box\phi &= \tilde{\nabla}_a\tilde{\nabla}^a\phi\ ,
\end{aligned}
$$

Properties: Second order dynamics both for the tensor and scalar
GWs (tensor perturbations) propagate with the speed of light

Constraints on Horndeski theory from GW170817

GW propagation speed agrees with the speed of light at the order of one part in quadrillionth at low redshifts

1. Theories with dependence of the kinetic term X in the coupling of the Ricci curvature R and Einstein tensor G_{mn} in L_4 and L_5 are disruled
2. L_5 does not depend on ϕ either (except through its derivatives)
3. due to the Bianchi identities, the whole L_5 vanishes

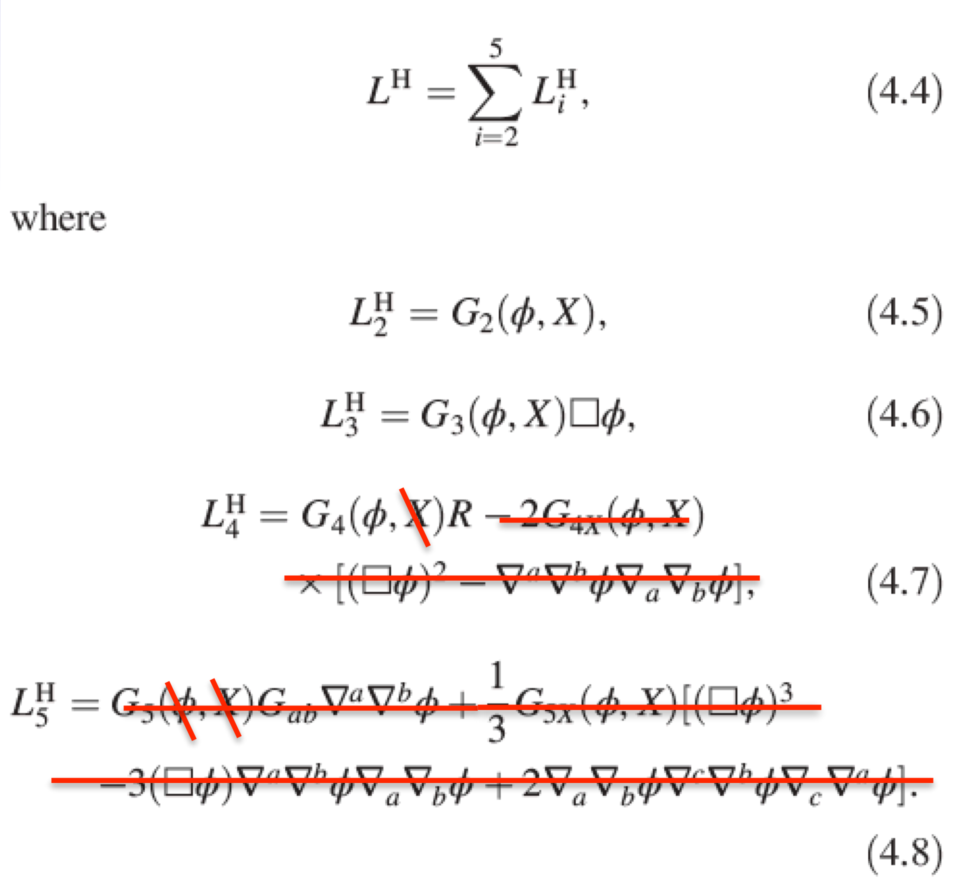

$$L^{\mathrm{H}} = \sum_{i=2}^{5} L_i^{\mathrm{H}}, \qquad (4.4)$$

where

$$L_2^{\mathrm{H}} = G_2(\phi, X), \qquad (4.5)$$

$$L_3^{\mathrm{H}} = G_3(\phi, X)\Box\phi, \qquad (4.6)$$

$$L_4^{\mathrm{H}} = G_4(\phi, \cancel{X})R \cancel{- 2G_{4X}(\phi, X)} \\ \cancel{\times [(\Box\phi)^2 - \nabla^a\nabla^b\phi\nabla_a\nabla_b\phi]}, \qquad (4.7)$$

$$L_5^{\mathrm{H}} = \cancel{G_5(\cancel{\phi}, \cancel{X})G_{ab}\nabla^a\nabla^b\phi + \frac{1}{3}G_{5X}(\phi, X)[(\Box\phi)^3} \\ \cancel{-3(\Box\phi)\nabla^a\nabla^b\phi\nabla_a\nabla_b\phi + 2\nabla_a\nabla_b\phi\nabla^c\nabla^b\phi\nabla_c\nabla^a\phi]}. \qquad (4.8)$$

Kobayashi, T.; Yamaguchi, M.; Yokoyama, J., Prog. Theor. Phys. 2011, 126, 511–529.
De Felice, A.; Tsujikawa, S., JCAP 2012, 007.
Baker, T.; Bellini, E.; Ferreira, P.G.; Lagos, M.; Noller, J.; Sawicki, I., Phys. Rev. Lett. 2017, 119, 251301.
Ezquiaga, J.M.; Zumalacarregu, M., Phys. Rev. Lett. 2017, 119, 251304.
Creminelli, P.; Vernizzi, F. Phys. Rev. Lett. 2017, 119, 251302.

LIGO, Virgo, and partners make first detection of gravitational waves and light from colliding neutron stars

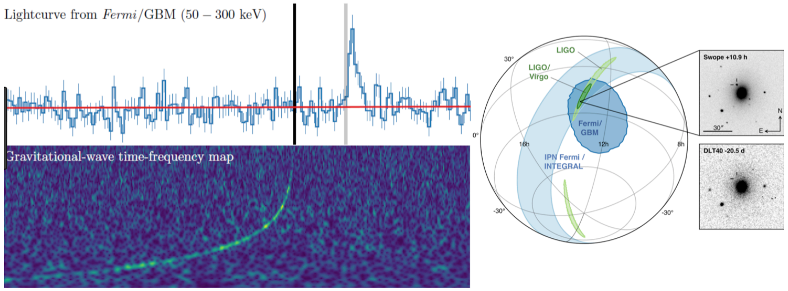

Stability analysis example: perturbations of spherically symmetric static BHs in scalar-tensor gravity

EFT action:

$$S^{EFT}=\int dx^4\sqrt{-\tilde{g}}L^{EFT}\left(N,M,\mathcal{K},\mathfrak{K},K,\varkappa,\mathcal{L}^*,L^*,\lambda^*,R;r\right)$$

"radial unitary" gauge

Scalars from embedding variables:

$$\mathfrak{K}\equiv\mathcal{K}^a\mathcal{K}_a\ ,\quad K\equiv K^a{}_a\ ,\quad \varkappa\equiv K^a{}_bK^b{}_a\ ,\quad L^*\equiv L^{*a}{}_a\ ,\quad \lambda^*\equiv L^{*a}{}_bL^{*b}{}_a$$

Variations to second order:

$$\begin{aligned}\delta S^{EFT} &= \delta_1S^{EFT}+\delta_2S^{EFT}\\ &= \int dx^4\Big(\delta_1\sqrt{-\tilde{g}}L^{EFT}+\sqrt{-\tilde{g}}\delta_1L^{EFT}\\ &\quad +\delta_1\sqrt{-\tilde{g}}\delta_1L^{EFT}+\delta_2\sqrt{-\tilde{g}}L^{EFT}+\sqrt{-\tilde{g}}\delta_2L^{EFT}\Big)\end{aligned}$$

variation of the metric determinant:

$$\begin{aligned}\delta\sqrt{-\tilde{g}} &= \delta_1\sqrt{-\tilde{g}}+\delta_2\sqrt{-\tilde{g}}\\ &= \sqrt{-\tilde{g}}\left(\frac{\delta_1N}{\bar{N}}+\frac{\delta_1M}{\bar{M}}+2\zeta\right)\\ &\quad +\sqrt{-\tilde{g}}\left[\frac{\delta_1M\delta_1N}{\bar{M}\bar{N}}+2\zeta\left(\frac{\delta_1N}{\bar{N}}+\frac{\delta_1M}{\bar{M}}\right)+2\zeta^2\right]\end{aligned}$$

conformal transformation between the 2-dimensional metrics:

$$g_{ab}=e^{2\zeta}\bar{g}_{ab}$$

conformal-factor

First order variation

Line element:

$$\boxed{\bar{N}^a = \bar{M}^a = \bar{\mathcal{N}} = 0} \longrightarrow ds^2 = -\bar{N}^2 dt^2 + \bar{M}^2 dr^2 + r^2 \left(d\theta^2 + \sin^2\theta d\varphi^2\right)$$

Background values of the variables in the action:

$$\bar{\mathcal{K}} = \bar{K} = \bar{\varkappa} = \bar{\mathfrak{K}} = 0 \,, \quad \bar{\mathcal{L}}^* = -\frac{\bar{N}'}{\bar{M}\bar{N}} \,, \quad \bar{L}^* = \frac{2}{\bar{M}r} \,, \quad \bar{\lambda}^* = \frac{2}{\bar{M}^2 r^2} \,, \quad \bar{R} = \frac{2}{r^2}$$

Nonvanishing first order variations (4 independent):

$$\underline{\delta_1 M}, \; \underline{\delta_1 N}\,, \; \delta_1 R = -2\underline{\zeta}\bar{R} - 2\bar{g}^{ab}\bar{D}_a\bar{D}_b\zeta \,, \; \delta_1\mathcal{K} = \mathcal{K} = \frac{1}{\bar{M}\bar{N}}\left[\partial_t\left(\delta_1 M\right) - \partial_r\left(\underline{\delta_1\mathcal{N}}\right)\right]$$

Vanishing ones (second order variations only): $\delta_1\varkappa = \delta_1\mathfrak{K} = 0$

Other (dependent) first order variations:

$$\begin{aligned} \delta_1\lambda^* &= \frac{2}{\bar{M}r}\delta_1 L^* \\ \delta_1 L^* &= \left[\tilde{\nabla}_a m^a - \frac{\bar{N}'}{\bar{M}\bar{N}} - \frac{2}{\bar{M}r}\right] + \delta_1\mathcal{L}^* \end{aligned}$$

$$\begin{aligned} \delta_1\mathcal{L}^* &= -\frac{\partial_r\left(\delta N\right)}{\bar{M}\bar{N}} + \frac{\bar{N}'}{\bar{M}\bar{N}}\left(\frac{\delta_1 M}{\bar{M}} + \frac{\delta_1 N}{\bar{N}}\right) \\ \delta_1 K &= K = \tilde{\nabla}_a n^a - \delta_1\mathcal{K} \end{aligned}$$

Equations of motion for the background

First order variation of the EFT action:

$$\begin{aligned}
\delta_1 S^{EFT} &= \int d^4x\sqrt{-\tilde{g}}\,\Big\{\,\big[L_N^{EFT}\delta_1 N + L_M^{EFT}\delta_1 M + L_{\mathcal{K}}^{EFT}\delta_1\mathcal{K} + L_K^{EFT}\delta_1 K \\
&\quad + L_{\mathcal{L}^*}^{EFT}\delta_1\mathcal{L}^* + L_{L^*}^{EFT}\delta_1 L^* + L_{\lambda^*}^{EFT}\delta_1\lambda^* + L_R^{EFT}\delta_1 R\big] + L^{EFT}\delta_1\ln\sqrt{-\tilde{g}}\Big\} \\
&= \text{.....cumbersome calculations ......} \\
&= \int d^4x\sqrt{-\tilde{g}}\left(\frac{\delta_1 S^{EFT}}{\delta\ln N}\delta\ln N + \frac{\delta_1 S^{EFT}}{\delta\ln M}\delta\ln M + \underline{\frac{\delta_1 S^{EFT}}{\delta\ln\mathcal{N}}\delta\ln\mathcal{N} +} \frac{\delta_1 S^{EFT}}{\delta\zeta}\delta\zeta\right) \\
&\quad + \text{total covariant divergencies}
\end{aligned}$$

Equations of motion:

$$\boxed{\begin{aligned}
\frac{\delta_1 S^{EFT}}{\delta\ln N} &= L^{EFT} + \bar{N}L_N^{EFT} + \frac{1}{\bar{M}}\left(\frac{2}{r} + \frac{\bar{N}'}{\bar{N}} + \partial_r\right)L_{\mathcal{L}^*}^{EFT} = 0 \\
\frac{\delta_1 S^{EFT}}{\delta\ln M} &= L^{EFT} + \bar{M}L_M^{EFT} - \frac{2}{r\bar{M}}\mathcal{F} + \frac{\bar{N}'}{\bar{M}\bar{N}}L_{\mathcal{L}^*}^{EFT} = 0 \\
\frac{\delta_1 S^{EFT}}{\delta\ln\mathcal{N}} &= \frac{1}{\bar{N}\bar{M}}\left[\partial_r L_{\mathcal{K}}^{EFT} + \frac{2}{r}\left(L_{\mathcal{K}}^{EFT} - L_K^{EFT}\right)\right] = 0 \\
\frac{\delta_1 S^{EFT}}{\delta\zeta} &= 2\left[L^{EFT} - \frac{1}{\bar{M}}\left(\frac{2}{r} + \frac{\bar{N}'}{\bar{N}} + \partial_r\right)\mathcal{F} - \frac{2}{r^2}L_R^{EFT}\right] = 0
\end{aligned}}$$

$$\partial_r\left(r^2 L_{\mathcal{K}}^{EFT}\right) = 2r\,L_K^{EFT}$$

arising from the non-orthogonality of the employed double foliation

Scalar perturbations for GLPV black holes: gauge fixing

Unambiguous gauge-fixing for scalar perturbations of both the metric tensor and scalar field on a spherically symmetric, static background.

C. Gergely, Z. Keresztes, L. Á. Gergely, *Gravitational dynamics in 2+1+1 decomposed space-time along nonorthogonal double foliations. Hamiltonian evolution and gauge fixing,* Phys. Rev. D 99, 104071 (2019)

Perturbed metric (overbar = unperturbed quantities):

$$
\begin{aligned}
ds^2 \;=\; & -\left(\bar{N}^2 + 2\bar{N}\delta N\right) dt^2 + 2\bar{M}\delta\mathcal{N} dt d\chi + 2\delta N_a dt dx^a \\
& + \left(\bar{g}_{ab} + \delta g_{ab}\right) dx^a dx^b + 2\delta M_a dx^a d\chi + \left(\bar{M}^2 + 2\bar{M}\delta M\right) d\chi^2
\end{aligned}
$$

Choices on the background:

R. Kase, L. Á. Gergely, S. Tsujikawa, *Effective field theory of modified gravity on the spherically symmetric background: Leading order dynamics and the odd-type perturbations* Phys. Rev. D 90, 124019 (2014)

$$\bar{N}^a = \bar{M}^a = 0$$

(evolutions perpendicular to $\Sigma_{t\chi}$)

$$\bar{\mathcal{N}} = 0$$

(perpendicular double foliation)

$$\bar{\phi} = \bar{\phi}(\chi)$$

(constant scalar field on $\bar{\mathfrak{M}}_\chi$)

Even/odd decomposition and transformation

Helmholz-type **decomposition** of the **shift vectors** and **metric tensor** into scalars (even), curl-free (even) and divergence-free (odd) parts:

$$
\begin{aligned}
\delta N_a &= \bar{D}_a P + E_a^b \bar{D}_b Q \\
\delta M_a &= \bar{D}_a V + E_a^b \bar{D}_b W \\
\delta g_{ab} &= \bar{g}_{ab} A + \bar{D}_a \bar{D}_b B + \\
& \frac{1}{2}\left(E_a^c \bar{D}_c \bar{D}_b + E_b^c \bar{D}_c \bar{D}_a\right) C
\end{aligned}
$$

$$E_{ab} = \sqrt{\bar{g}}\varepsilon_{ab} \,, \qquad \varepsilon_{\theta\varphi} = 1$$

Transformations of the metric and scalar **under diffeomorphisms:**

(overhat = perturbation after diffeomorphism)

$$
\begin{aligned}
\mathfrak{L}_\xi \tilde{g}_{ab} &= \delta\tilde{g}_{ab} - \widehat{\delta\tilde{g}_{ab}} \\
\mathfrak{L}_\xi \phi &= \delta\phi - \widehat{\delta\phi} \\
(\xi^t, \xi^\chi, \xi^a &= \bar{D}^a \xi + E^{ba} \bar{D}_b \eta)
\end{aligned}
$$

in detail

$$
\begin{aligned}
\widehat{\delta\phi} &= \delta\phi - \bar{\phi}' \xi^\chi \\
\widehat{\delta N} &= \delta N - \bar{N}\dot{\xi}^t - \bar{N}'\xi^\chi \,, \\
\widehat{\delta \mathcal{N}} &= \delta \mathcal{N} - \frac{\bar{N}^2}{2\bar{M}}\xi^{t\prime} + \frac{\bar{M}}{2}\dot{\xi}^\chi \,, \\
\widehat{\delta M} &= \delta M + \bar{M}'\xi^\chi + \bar{M}\xi^{\chi\prime} \,, \\
\widehat{P} &= P - \bar{N}^2 \xi^t + \dot{\xi} \,, \\
\widehat{Q} &= Q + \dot{\eta} \,, \\
\widehat{V} &= V + \bar{M}^2 \xi^\chi + \xi' - \frac{2}{\chi}\xi \,, \\
\widehat{W} &= W + \eta' - \frac{2}{\chi}\eta \,, \\
\widehat{A} &= A + \frac{2}{\chi}\xi^\chi \,, \\
\widehat{B} &= B + 2\xi \,, \\
\widehat{C} &= C + 2\eta \,.
\end{aligned}
$$

Gauge choice

$\rightarrow \quad \xi^{\chi}$ to fix $\widehat{\delta\phi} = 0$

perturbation of 2D-metric = **conformal rescaling**

$$\left.\begin{array}{l} \rightarrow \quad \xi \text{ to fix } \widehat{B} = 0 \\ \rightarrow \quad \eta \text{ to fix } \widehat{C} = 0 \end{array}\right\} \longrightarrow \boxed{\widehat{g}_{ab} \;=\; (1+\widehat{A})\bar{g}_{ab}}$$

Choice of ξ^t : (1) for orthogonal foliation $\rightarrow$ to fix $\widehat{\delta\mathcal{N}} = 0$

$$\xi^t = \int d\chi \frac{2\bar{M}}{\bar{N}^2}\left(\delta\mathcal{N} + \frac{\bar{M}}{2}\dot{\xi}^{\chi}\right) + F(t,\theta,\varphi)$$

contains an arbitrary function,
hampering the physical interpretation of perturbations

(2) for non-orthogonal foliations $\rightarrow$ to fix $\widehat{P} = 0$

unambiguous gauge-choice:

$$\boxed{\xi^t = \frac{P+\dot{\xi}}{\bar{N}^2}\,, \qquad \xi^{\chi} = \frac{\delta\phi}{\bar{\phi}'}\,, \qquad \xi = -\frac{B}{2}\,, \qquad \eta = -\frac{C}{2}}$$

After gauge-fixing the discussion of perturbations possible

even sector: $\widehat{V}, \underbrace{\widehat{A}, \widehat{\delta N}, \widehat{\delta\mathcal{N}}, \widehat{\delta M}}_{\text{(only they have first order contributions)}}$ odd sector: $\widehat{Q}, \widehat{W}$

Zerilli-type Regge-Wheeler-type

F. Zerilli, Phys. Rev. D **9**, 860 (1974) T. Regge, J. A. Wheeler, Phys. Rev. **108**, 1063 (1957)

Comparison of gauge choices

RW

T. Regge, J. A. Wheeler, Stability of a Schwarzschild Singularity, Phys. Rev. 108, 1063 (1957).

GR, time-independent Schrödinger-equation with an effective potential

→ Stable w.respect to perturbations

KMS

T. Kobayashi, H. Motohashi, T. Suyama, Black hole perturbation in the most general scalar-tensor theory with second-order field equations I: The odd-parity sector, Phys. Rev. D 85, 084025 (2012) [arXiv:1202.4893 [gr-qc]].

T. Kobayashi, H. Motohashi, T. Suyama, Black hole perturbation in the most general scalar-tensor theory with second-order field equations II: the even-parity sector, Phys. Rev. D 89, 084042 (2014) [arXiv:1402.6740 [gr- qc]].

Horndeski, stability analysis, only 3 RW variables

KGT

R. Kase, L. Á. Gergely, S. Tsujikawa, Effective field theory of modified gravity on spherically symmetric background: leading order dynamics and the odd mode perturbations, Phys. Rev. D 90, 124019 (2014) [arXiv:1406.2402 [hep-th]].

EFT, odd sector stability analysis, nonphysical variables in the even sector

GKG

C. Gergely, Z. Keresztes, L. Á. Gergely, Gravitational dynamics in 2+1+1 decomposed space-time along nonorthogonal double foliations. Hamiltonian evolution and gauge fixing, Phys. Rev. D, megjelenés alatt (2019).

EFT, 4 RW variables + 1 d.o.f. due to the scalar

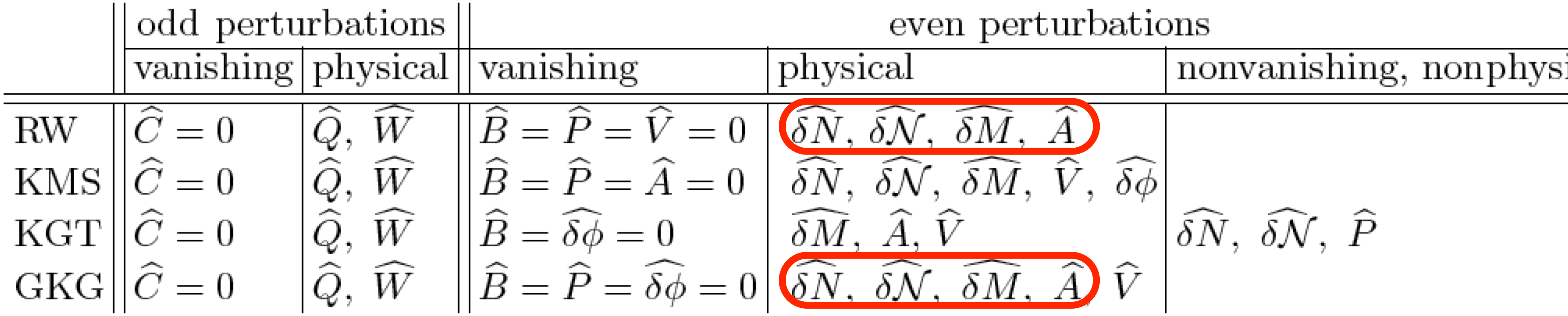

	odd perturbations		even perturbations		
	vanishing	physical	vanishing	physical	nonvanishing, nonphysi
RW	$\widehat{C}=0$	$\widehat{Q},\ \widehat{W}$	$\widehat{B}=\widehat{P}=\widehat{V}=0$	$\widehat{\delta N},\ \widehat{\delta\mathcal{N}},\ \widehat{\delta M},\ \widehat{A}$	
KMS	$\widehat{C}=0$	$\widehat{Q},\ \widehat{W}$	$\widehat{B}=\widehat{P}=\widehat{A}=0$	$\widehat{\delta N},\ \widehat{\delta\mathcal{N}},\ \widehat{\delta M},\ \widehat{V},\ \widehat{\delta\phi}$	
KGT	$\widehat{C}=0$	$\widehat{Q},\ \widehat{W}$	$\widehat{B}=\widehat{\delta\phi}=0$	$\widehat{\delta M},\ \widehat{A},\ \widehat{V}$	$\widehat{\delta N},\ \widehat{\delta\mathcal{N}},\ \widehat{P}$
GKG	$\widehat{C}=0$	$\widehat{Q},\ \widehat{W}$	$\widehat{B}=\widehat{P}=\widehat{\delta\phi}=0$	$\widehat{\delta N},\ \widehat{\delta\mathcal{N}},\ \widehat{\delta M},\ \widehat{A}\ \ \widehat{V}$	

Odd sector analysis: Q, W

Odd sector unaffected by the arbitrary function F, has been discussed in the framework of the orthogonal double foliation:

R. Kase, L. Á. Gergely, S. Tsujikawa, *Effective field theory of modified gravity on the spherically symmetric background: Leading order dynamics and the odd-type perturbations* Phys. Rev. D 90, 124019 (2014)

4th order equations for the evolution of perturbations:

$$\bar{D}^2\Psi^{(1)} = 0, \qquad \Psi^{(1)} \equiv a_1 \frac{\partial}{\partial t}\left(\dot{W} - Q' + \frac{2Q}{r}\right) + (a_3\bar{D}^2 - a_4)W,$$

$$\bar{D}^2\Psi^{(2)} = 0, \qquad \Psi^{(2)} \equiv \frac{1}{\sqrt{-\bar{g}}}\frac{\partial}{\partial r}\left[\sqrt{-\bar{g}}a_1\left(\dot{W} - Q' + \frac{2}{r}Q\right)\right] - a_2\left(\bar{D}^2 + \frac{2}{r^2}\right)Q.$$

where:

$$a_1 = \frac{L_{\mathfrak{K}}^{\mathrm{EFT}}}{4\bar{N}^2\bar{M}^2}, \qquad a_2 = \frac{L_{\varkappa}^{\mathrm{EFT}}}{2\bar{N}^2}, \qquad a_3 = \frac{L_{\lambda}^{\mathrm{EFT}}}{2\bar{M}^2}, \qquad a_4 = L_{\mathfrak{M}}^{\mathrm{EFT}} - \frac{2}{r^2}a_3.$$

Multipolar decomposition

Decomposition in terms of spherical harmonics:

$$\Psi^{(i)}(t,r,\theta,\varphi) = \sum_{l,m} \Psi^{(i)}_{lm}(t,r) Y_l^m.$$

Reduce the differential order to 2 by exploring the identities:

$$r^2 \bar{D}^2[\Psi^{(i)}_{lm}(t,r)Y_l^m] + l(l+1)[\Psi^{(i)}_{lm}(t,r)Y_l^m] = 0.$$

2nd order system for each mode: $f_l \equiv \sum_m f_{lm} Y_l^m$

2nd order time derivative -> dynamical eq.

$$\sum_l l(l+1)\Psi^{(1)}_l = 0, \qquad \Psi^{(1)}_l \equiv a_1 \frac{\partial}{\partial t}\left(\dot{W}_l - Q'_l + \frac{2}{r}Q_l\right) - \left[a_3 \frac{l(l+1)}{r^2} + a_4\right] W_l,$$

$$\sum_l l(l+1)\Psi^{(2)}_l = 0, \qquad \Psi^{(2)}_l \equiv \frac{1}{\sqrt{-\bar{g}}}\frac{\partial}{\partial r}\left[\sqrt{-\bar{g}}\, a_1 \left(\dot{W}_l - Q'_l + \frac{2}{r}Q_l\right)\right] + a_2 \frac{l(l+1)-2}{r^2} Q_l.$$

1st order time derivative —> Lagrangian constraint

Monopolar, dipolar, higher-order modes

Monopolar mode: trivial, appear only in total divergences in Lag.

Dipolar mode: non-dynamical, constant in time

Higher order mode solutions parametrically given as:

$$Q_l = -\frac{r^2}{a_2(l+2)(l-1)\sqrt{-\bar{g}}}\frac{\partial}{\partial r}\left(\sqrt{-\bar{g}}a_1 Z_l\right) \qquad W_l = \frac{a_1 r^2}{a_3 l(l+1) + a_4 r^2}\dot{Z}_l,$$

Second-order correction in the Lagrangian:

$$\delta_2\mathcal{L}_l^{\rm odd} = \frac{l(l+1)}{(l+2)(l-1)}\sqrt{-\bar{g}}\left[\boxed{-\frac{a_1^2}{a_3}\dot{Z}_l^2} - \frac{a_1^2}{a_2}Z_l'^2 - a_1(\bar{D}Z_l)^2 - U^{\rm H}(r)Z_l^2 + \frac{a_1}{a_3}L_{\mathfrak{M}}^{\rm EFT}W_l\dot{Z}_l\right]$$

last term is l-dependent

—> $\boxed{L_{\mathfrak{M}}^{\rm EFT} = 0.}$ to avoid propagation speed to be dependent (holds in both Horndeski and GLPV)

where the potential $U^{\rm H}(r)$ is given by

$$U^{\rm H}(r) = -a_1\frac{\partial}{\partial r}\left[\frac{1}{\sqrt{-\bar{g}}a_2}\frac{\partial}{\partial r}\left(\sqrt{-\bar{g}}a_1\right)\right] - \frac{2a_1}{r^2}.$$

Ghost modes, stability analysis

- Condition to avoid scalar ghosts: $\boxed{L_{\lambda}^{\mathrm{EFT}} < 0.}$
- Dispersion relations in the radial direction and along the sphere in the high-frequency / geometrical optics / large wave number limit

$$\omega^2 + \frac{a_3}{a_2} k_r^2 = 0, \qquad \omega^2 + \frac{a_3}{a_1} k_\Omega^2 = 0,$$

- Sound velocity-squares :

(defined as change of tortoise coordinate in proper time)

$$c_r^2 \equiv \frac{\bar{M}^2 k_r^2}{\bar{N}^2 \omega^2} = -\frac{\bar{M}^2 a_3}{\bar{N}^2 a_2} = \boxed{-\frac{L_{\lambda}^{\mathrm{EFT}}}{L_{\varkappa}^{\mathrm{EFT}}},}$$

$$c_\Omega^2 \equiv \frac{k_\Omega^2}{\bar{N}^2 \omega^2} = -\frac{a_3}{\bar{N}^2 a_1} = \boxed{-\frac{2L_{\lambda}^{\mathrm{EFT}}}{L_{\mathfrak{K}}^{\mathrm{EFT}}}}$$

- Conditions to avoid Laplacian instabilities:

$$\boxed{L_{\varkappa}^{\mathrm{EFT}} > 0, \qquad L_{\mathfrak{K}}^{\mathrm{EFT}} > 0.}$$

$$\begin{aligned} &\mathcal{R} \equiv {}^{(2)}R^a{}_a, \qquad \mathfrak{M} \equiv M_a M^a, \qquad \mathfrak{K} \equiv \mathcal{K}_a \mathcal{K}^a = \mathcal{L}_a \mathcal{L}^a, \\ &K \equiv K^a{}_a, \qquad \varkappa \equiv K^a{}_b K^b{}_a, \qquad L \equiv L^a{}_a, \\ &\lambda \equiv L^a{}_b L^b{}_a. \end{aligned} \tag{3.2}$$

- was applied to both covariantized and covariant galileon models

Summary

- We reestablished the full gauge invariance, by exploring a non-orthogonal double foliation. Generic discussion of perturbations is now possible.
- We geometrically interpreted the 10th metric variable as
  (1) the angle of the Lorentz-rotation of the basis vectors,
  (2) the measure of the vorticity of the basis vectors.
- We identified those geometrical quantities characterising the embedding, which bear dynamical role (they contain time-derivatives).
- For scalar-tensor gravitational theories we worked out an unambiguous gauge fixing for spherically symmetric static black hole perturbations, applicable for both the even and odd sectors.
- We derived the first order variations of an EFT action for spherically symmetric static background and obtained the equations of motion for the background
- We completed the discussion of the odd modes of perturbations, including stability analysis
- Full second order variation and discussion of the even modes — in progress

Prospects

1. *Could the Event Horizon Telescope distinguish between general relativistic and modified gravity black holes?*

Not yet. (Cannot distinguish various black holes / accretion parameters in μas resolution not even in general relativity)

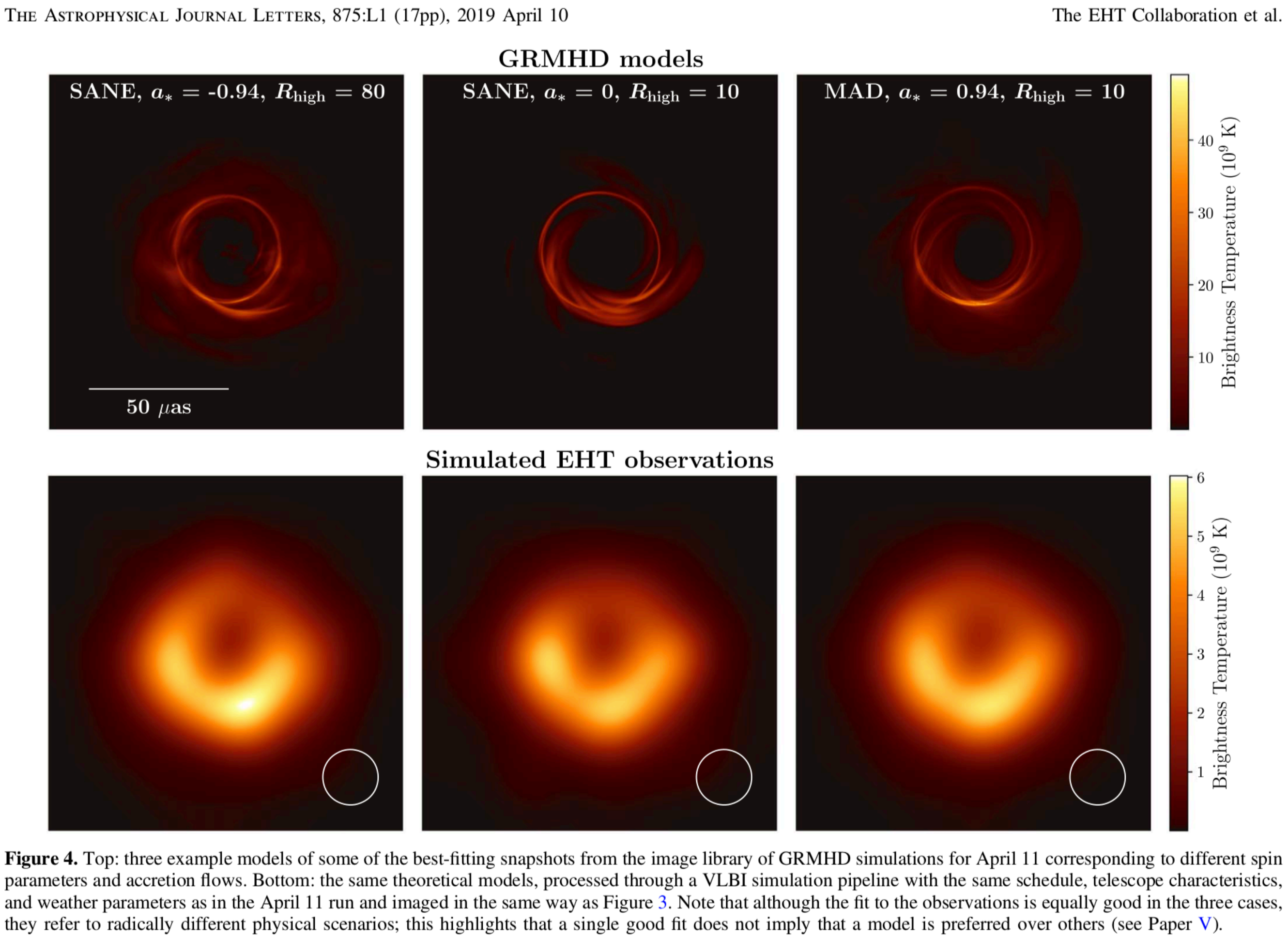

The Astrophysical Journal Letters, 875:L1 (17pp), 2019 April 10 The EHT Collaboration et al.

Figure 4. Top: three example models of some of the best-fitting snapshots from the image library of GRMHD simulations for April 11 corresponding to different spin parameters and accretion flows. Bottom: the same theoretical models, processed through a VLBI simulation pipeline with the same schedule, telescope characteristics, and weather parameters as in the April 11 run and imaged in the same way as Figure 3. Note that although the fit to the observations is equally good in the three cases, they refer to radically different physical scenarios; this highlights that a single good fit does not imply that a model is preferred over others (see Paper V).

Prospects

2. *Can distinguish gravitational wave detection between general relativistic and modified gravity black holes?*

In the future yes. (Third generation detectors)

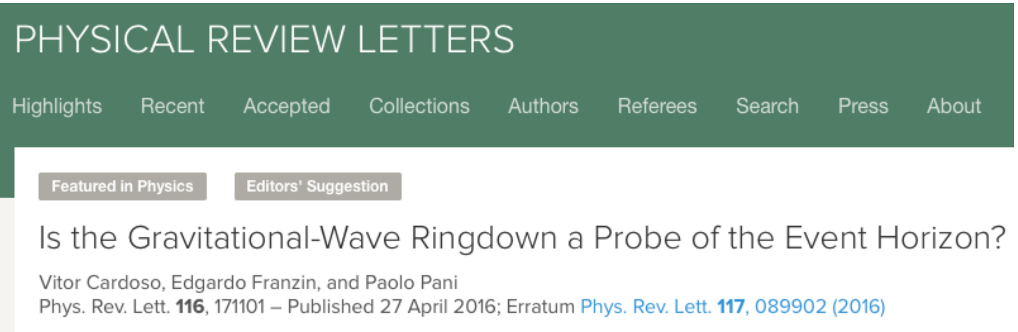

PHYSICAL REVIEW LETTERS

Highlights Recent Accepted Collections Authors Referees Search Press About

Featured in Physics Editors' Suggestion

Is the Gravitational-Wave Ringdown a Probe of the Event Horizon?

Vitor Cardoso, Edgardo Franzin, and Paolo Pani
Phys. Rev. Lett. **116**, 171101 – Published 27 April 2016; Erratum Phys. Rev. Lett. **117**, 089902 (2016)

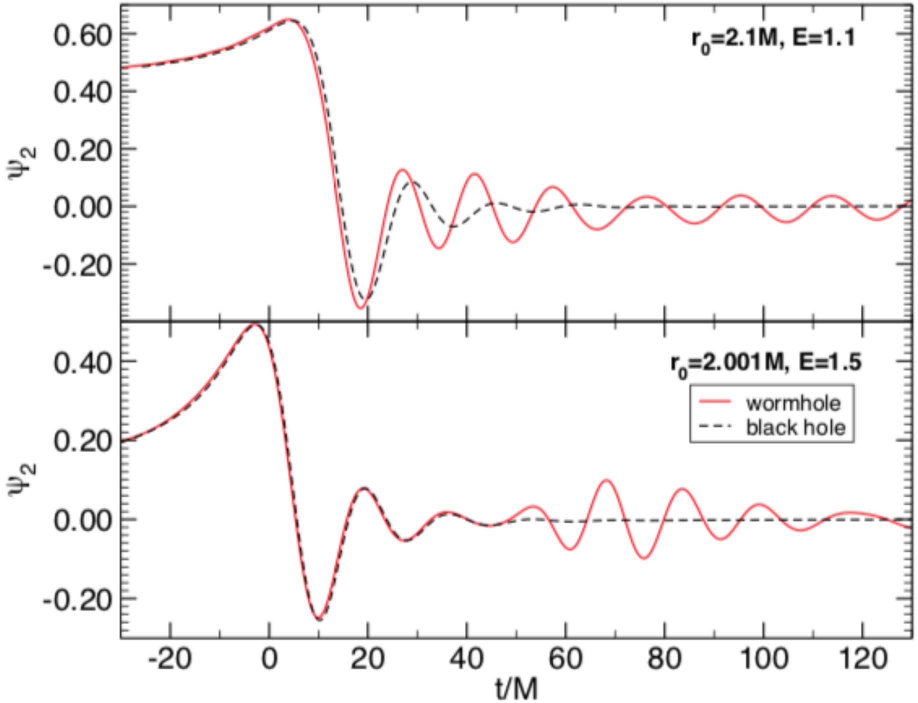

PHYSICAL REVIEW D

covering particles, fields, gravitation, and cosmology

Highlights Recent Accepted Authors Referees Search Press About

Quasinormal modes of black holes in Horndeski gravity

Oliver J. Tattersall and Pedro G. Ferreira
Phys. Rev. D **97**, 104047 – Published 25 May 2018

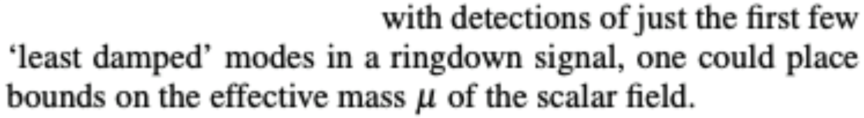

with detections of just the first few 'least damped' modes in a ringdown signal, one could place bounds on the effective mass μ of the scalar field.

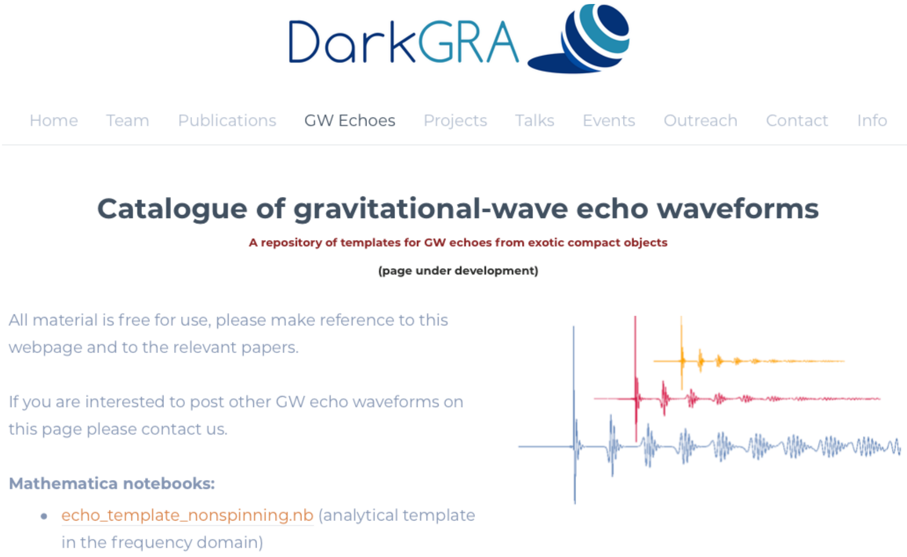

DarkGRA

Home Team Publications GW Echoes Projects Talks Events Outreach Contact Info

Catalogue of gravitational-wave echo waveforms

A repository of templates for GW echoes from exotic compact objects

(page under development)

All material is free for use, please make reference to this webpage and to the relevant papers.

If you are interested to post other GW echo waveforms on this page please contact us.

Mathematica notebooks:

- echo_template_nonspinning.nb (analytical template in the frequency domain)

https://www.darkgra.org/gw-echo-catalogue.html?fbclid=IwAR0eviY1f6TV2G1Ft4P8OkSEilhRlsEmzEiG2B0b3HUjNFu0Bq31lB_gNd8